Plasma Physics and Controlled Fusion

PAPER

On improved confinement in mirror plasmas by a radial electric field

To cite this article: O Ågren and V E Moiseenko 2017 *Plasma Phys. Control. Fusion* **59** 115001

IOP Publishing Plasma Physics and Controlled Fusion

Plasma Phys. Control. Fusion **59** (2017) 115001 (22pp) https://doi.org/10.1088/1361-6587/aa8544

On improved confinement in mirror plasmas by a radial electric field

O Ågren[1] and V E Moiseenko[2]

[1] Uppsala University, Ångström laboratory, Box 534, SE-751 21 Uppsala, Sweden
[2] Institute of Plasma Physics, National Science Center, Kharkov Institute of Physics and Technology, Akademichna st. 1, 61108 Kharkiv, Ukraine

E-mail: Olov.Agren@angstrom.uu.se

Received 27 January 2017, revised 30 July 2017
Accepted for publication 9 August 2017
Published 18 September 2017

Abstract

A weak radial electric field can suppress radial excursions of a guiding center from its mean magnetic surface. The physical origin of this effect is the smearing action by a poloidal $\mathbf{E} \times \mathbf{B}$ rotation, which tend to cancel out the inward and outward radial drifts. A use of this phenomenon may provide larger margins for magnetic field shaping with radial confinement of particles maintained in the collision free idealization. Mirror fields, stabilized by a quadrupolar field component, are of particular interest for their MHD stability and the possibility to control the quasi neutral radial electric field by biased potential plates outside the confinement region. Flux surface footprints on the end tank wall have to be traced to avoid short-circuiting between biased plates. Assuming a robust biasing procedure, moderate voltage demands for the biased plates seems adequate to cure even the radial excursions of Yushmanov ions which could be locally trapped near the mirrors. Analytical expressions are obtained for a magnetic quadrupolar mirror configuration which possesses minimal radial magnetic drifts in the central confinement region. By adding a weak controlled radial quasi-neutral electric field, the majority of gyro centers are predicted to be forced to move even closer to their respective mean magnetic surface. The gyro center radial coordinate is in such a case an accurate approximation for a constant of motion. By using this constant of motion, the analysis is in a Vlasov description extended to finite β. A correspondence between that Vlasov system and a fluid description with a scalar pressure and an electric potential is verified. The minimum B criterion is considered and implications for flute mode stability in the considered magnetic field is analyzed. By carrying out a long-thin expansion to a higher order, the validity of the calculations are extended to shorter and more compact device designs.

Keywords: radial invariant, radial electric field, biased potential plates, magnetic mirror, mirror machine, hybrid reactor, minimum B

1. Introduction

The paper studies a mirror confinement scheme, where each particle is moving close to its mean magnetic surface. A tool to achieve this is a quasi-neutral radial electric field. The physical origin of this effect is the smearing action by a poloidal $\mathbf{E} \times \mathbf{B}$ rotation, which tend to be effective for a distinct cancelation of the inward and outward radial drifts. Although margins for tolerable field errors in the magnetic field design may increase with a radial electric field, it is still essential to select the magnetic field with some care. Gross MHD instabilities should be avoided, as well as too strong radial magnetic drifts. For a minimum B mirror field, the ellipticity of the flux tubes need also to be kept within a tolerable range. We here consider a single cell mirror, with a quadrupolar field component to provide gross MHD stability.

A fusion plasma needs an almost perfect confinement of the charges in the collision free idealization [1, 2]. Constants of motions are useful to identify confinement properties. In a collision free idealization, it is well known that longitudinal

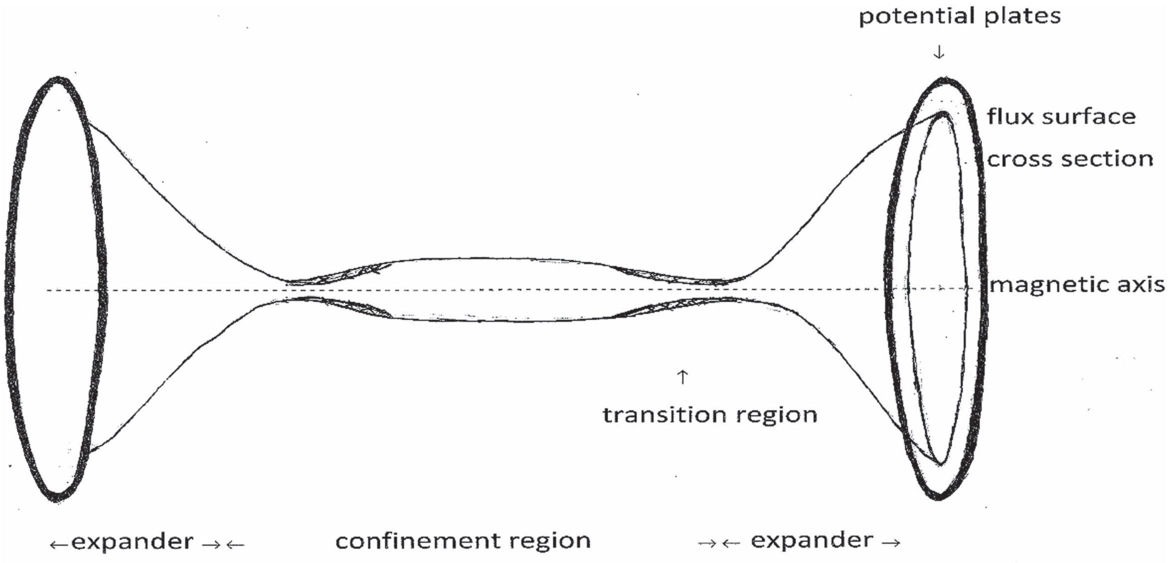

Figure 1. Overview of mirror magnetic field, expander region and arrangement of biased potential plates at end tank wall. It is essential to trace flux tube cross sections at the end tank for the geometrical design of the insulation between the biased plates. Magnetic fields can be constructed where these flux tube cross sections are almost circular. The purpose is to control a radial variation of the quasi-neutral electric potential and plasma rotation at the confinement region by the potentials at the biased plates. An annular transition region where neoclassical effects can be important is indicated in the figure.

confinement is based on two constants of motion, namely the magnetic moment $\mu(\mathbf{x}, \mathbf{v})$ and the energy $\varepsilon(\mathbf{x}, \mathbf{v})$ of the particle:

$$\mu = \frac{mv_\perp^2}{2B}, \ \varepsilon = q\phi + \mu B + \frac{m}{2}v_\parallel^2.$$

Here, q, m, B, ϕ, $v_\perp$ and $v_\parallel$ are the charge, mass, magnetic field modulus, electric potential and speed along and perpendicular to the magnetic field. The mirror effect then forces the particle motion to be limited to a region bounded by a magnetic field strength

$$B < \frac{\varepsilon - q\phi}{\mu} \approx \frac{\varepsilon}{\mu},$$

where the last end assumes that the longitudinal variations of the electric potential are small. This would assure longitudinal confinement if each guiding center is restricted to move close to a single magnetic surface, but in most field configurations, a perpendicular drift can ruin confinement by a transverse motion into regions not intended for confinement. A goal of this paper is to approach a situation where most of the guiding center move close to their respective mean magnetic surface. Since a magnetic surface is labeled by a constant value of the radial Clebsch coordinate $r_0(\mathbf{x})$ (which determines the magnetic flux inside the magnetic surface), the radial coordinate $\bar{r}_0(\mathbf{x}, \mathbf{v})$ of the guiding center is an approximate constant of motion if the particle orbit remains close to its mean magnetic surface, i.e. (compare [3–5]).

Here, $r_0(\mathbf{x})$ is the radial Clebsch coordinate of the particle and $r_{0,g}(\mathbf{x}, \mathbf{v})$ is the small but fast 'gyro ripple' associated with the gyro oscillations of the particle around the magnetic field (this gyro ripple is responsible for the diamagnetic current, and the radial invariant enables descriptions of radial variations of the density and other quantities in the confinement scheme). A radial invariant in this form *does not exist* in typical confinement schemes (in toroidal devices, finite banana widths is one of the obstacles). A main objective of this paper is to analyze if that situation could be approached in mirror geometry, where a quasi-neutral electric field may assist to force the particles to move close to a magnetic surface (some conditions for quadrupolar mirror fields will be of special interest for this paper). Conditions for omnigenuity has over several decades been studied by many researchers. This paper pay a stronger attention on possibilities with of a radial electric electric field. This is outlined in figure 1. With a radial variation of the quasi-neutral electric potential, the plasma is forced to rotate. This response is based on a *plasma polarization effect*, for which Baker and Hammel [6] did pioneering studies.

To describe the plasma polarization phenomenon, it is instructive to first recall the motion of a single point charge moving from a field-free region into a region with constant magnetic field with a direction perpendicular to the initial velocity $\mathbf{v}$ of the charge. In the magnetic field region, the resulting orbit is a semi-circle, and the charge is reflected back to the field free region in the opposite velocity direction, where positive and negative charges bend in opposite directions along their semicircles in the magnetic field region. In such a single particle description, penetration into the magnetic field region is clearly not possible. As described by Baker and Hammel, the situations is different for a collision-free plasma beam of sufficient density entering a magnetic field region. On the entrance, electrons are slightly displaced by the Lorentz force where the charge displacement produces a perpendicular electric field, which they refers to as a plasma polarization mechanism. The magnitude of the electric field is (apart from possible pressure gradient effects) determined by the condition that the electric field in the co-moving beam

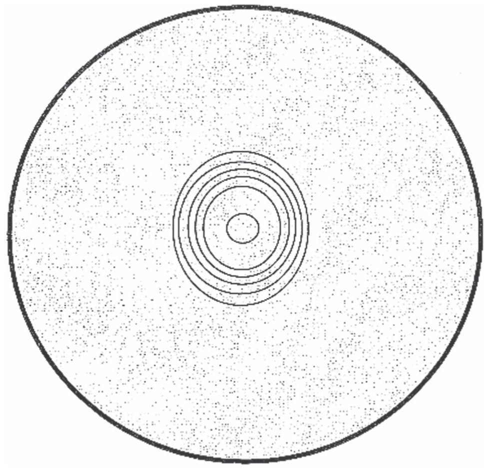

Figure 2. Sketch of cross sections of flux tubes at the end tank. There is a slight deviation from circles of these curves. This has to be considered for the shapes of the biased plates to avoid short-circuiting between flux surfaces. With quadrupolar symmetry, the flux surface footprints at the end tank on the opposite side is rotated by 90°. The flux surface cross section prints at the wall are to leading order mapped to circles at the mid plane. The flux tube expansion may be envisioned as a 'lens tool' to magnify the radial scale length at the confinement region, with a magnification $\sqrt{B_0/B_{\text{end tank}}} \approx 10$ given by the square root of the ratio between the magnetic field strengths at the mid plane to the end tank value. Short-circuiting of adjacent biased potential plates by the high electron mobility along flux surfaces must be avoided, which gives constraints on electric isolation widths and the number of independent biased potentials (see appendix D). Magnetic shaping is crucial for this.

system is zero, whereby

$$\mathbf{E} + \mathbf{v} \times \mathbf{B} = 0.$$

This result for the electric field in the lab system is consistent with the same beam velocity in the field-free and magnetic field regions. A short calculation gives the result $\mathbf{v} = (\mathbf{E} \times \mathbf{B})/B^2$ for the plasma velocity in the magnetic field region, i.e. the plasma polarization results in a conventional $\mathbf{E} \times \mathbf{B}$ drift [6]. The situation described here assumes that the magnetic field lines intersect insulating plates. If these plates are replaced by conducting plates, the plasma polarization is short-circuited by the high electron mobility along magnetic field lines, and plasma beam penetration cannot occur [6].

We are here interested in the reverse action, i.e. to produce a plasma motion (a rotation in our case) by a quasi-neutral electric field across the magnetic field. An arrangement of biased potential plates at the end tank wall may be an arrangement to control the quasi-neutral electric field in the plasma, as depicted in figures 1 and 2. For this scheme it is essential that the region between the mirrors and the end tank wall contains a low density quasi-neutral plasma (with a diminishingly small Debye screening length), where the high electron mobility along magnetic field lines tend to relax potential variations along the magnetic surfaces (although some potential variations along flux surfaces can result from anisotropic pressure gradients, the mirror effect, collisions or drifts, a conjecture is that in the simplest model, each flux surface corresponds to a short-circuited region).

The goal is transpose a voltage difference between biased plates at the end tank to a similar voltage difference between flux surfaces in the confinement region. The biased potentials would then offer a control tool for the poloidal plasma rotation. A pre-ionized quasi-neutral plasma is assumed to fill the vacuum chamber before applying the biased potentials. The magnetic field with a quadrupolar component is arranged by a coil system, depicted in figure 3, which is capable of producing nearly circular cross sections of the magnetic surfaces at the end tank wall (the flux surface footprint on the expander wall has to be considered in the biased end plate geometrical arrangements to avoid short-circuiting). It is essential that the magnetic axis intersect the most central biased plate. With charged particles drifting close to a magnetic surface, our analysis predicts that a quasi-neutral electric potential, derived from the Vlasov equation, imply an $\mathbf{E} \times \mathbf{B}$ drift primarily in a poloidal direction.

To describe the implications for a radial electric in some more detail, we need to choose a magnetic field. We consider a long-thin expansion for a mirror field with almost straight magnetic field lines in the confinement region, stabilized by a quadrupolar magnetic field which produces a minimum B state to leading order. In the leading order, the magnetic field is the straight field line mirror (SFLM) field [7, 8]. The long-thin expansion [9] is here carried out to higher order with a goal to minimize radial magnetic drifts. One intention of the study is to enable more compact and shorter designs of the magnetic mirror device.

The magnetic field investigated here has certain favorable confinement properties (but also a certain drawback with a singular magnetic field strength, which will be briefly analyzed in the paper). Existence of a constant of motion for the magnetic drift motion provides a bounded radial motion for particles in the central confinement region, and radial excursion of the guiding centers from their mean flux surface are small. The situation is predicted to be further improved by adding a controlled radial electric field [5]. With very modest values of biased potentials generating the electric field in the plasma, radial drift excursions are predicted to decrease, and a majority of each gyro centers move almost arbitrarily close to their respective mean magnetic surface. This corresponds to the existence of a constant of motion, a radial invariant, which restricts the motion of a gyro center to the neighborhood of its mean flux surface. This radial invariant can be used to extend the analysis to finite beta Vlasov equilibria. Relations between such Vlasov systems and a fluid equilibria will be demonstrated.

Results in mirror machine research have undergone impressive progress during the last decades. Particularly important developments have been made on the electron temperature, which by many fusion researchers have been believed to be a showstopper for mirror fusion devices. The Budker Institute at Novosibirsk in Russia has a comprehensive experimental activity on axisymmetric mirrors. The Gol-3 device, containing a thin very high density plasma which is heated by a relativistic electron beam, was in the year 2002 turned into a multi-mirror with 26 cells [10]. The resulting electron temperature, around 1.5 keV, was a first dramatic demonstration that that mirror machines could reach

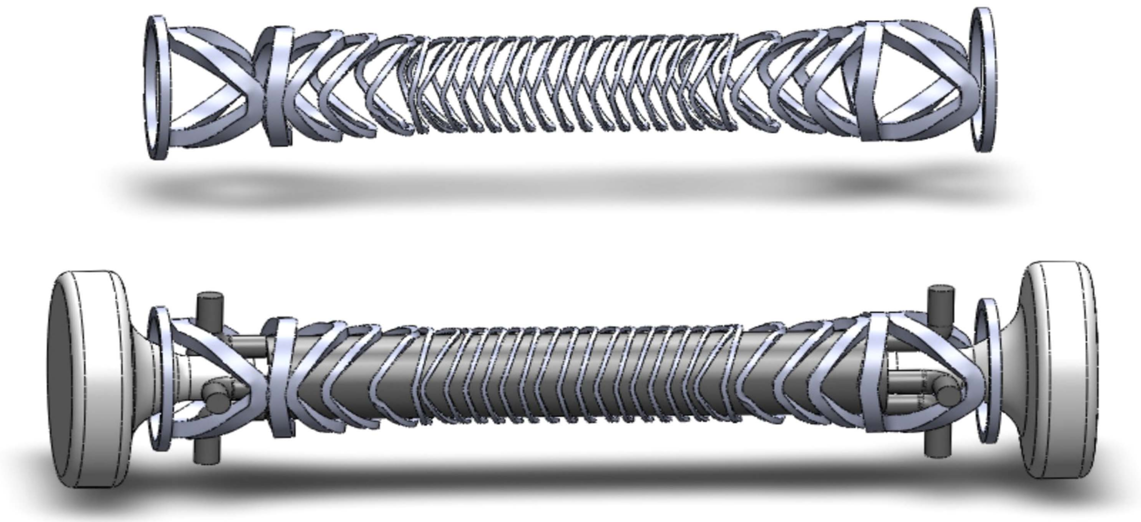

Figure 3. Shape of 3D superconducting coils aimed for a long-thin version of the SFLM field. Inner radius of the coils is 2.1 m and the outer radius is 2.89 m. With a vacuum chamber radius of 1 m, this provides sufficient space for a reactor blanket in between the vacuum chamber and the inner radius of the coils. Parameters are mid plane plasma radius $a = 0.4$ m, length of confinement region 25 m, and $B_0 = 1.5$ T. The SFLM field is reproduced by the coils in a confinement region with a mirror ratio $R_m \leqslant 4$, and beyond that confinement region the flux tube recirculates and expands towards the end tank walls with a final radius of 4 m (with almost circular cross section near the end tank). That provides large areas for plasma receiving plates (which correspond to the divertor plates in toroidal devices) and a power deposition below 1 MW m^{-2}, which is predicted to be within tolerable limits. The lower figure indicates locations of reactor blanket and inlets for coolant loops in a hybrid reactor design. No holes are Required in the envelope surface if feeding of fuel and heating and diagnostics are made through the mirror ends. Reactor engineering is simplified by the avoidance of such holes.

higher electron temperatures than expected from earlier experimental results in mirrors. The Gamma10 tandem mirror device at Tsukuba in Japan increased the electron temperature to about 650 eV (measured by soft x-ray spectroscopy) [11]. The gas dynamic trap (GDT) experiment at the Budker Institute at Novosibirsk achieved a doubling of the electron temperature to about 230 eV after introducing biased potential plates in the device [12]. More recently, the electron temperature in GDT (measured by Thompson scattering) has been increased to 660 eV and even reached about 900 eV in a few shots [13], in experiments where electron cyclotron resonance heating (ECRH) was applied in addition to the neutral beam heating. The achieved electron temperature in GDT is already of a practical interest for a fusion neutron source. A new axisymmetric device, which is a multicell 'tandem-mirror' modification of the single cell GDT, is under construction at the Budker Institute [14]. The construction of this new axisymmetric device has been motivated by the progress made on the axisymmetric Gol-3 and GDT devices.

An advantage of axisymmetric mirrors is the simple coil structure and flexibility to make modifications [15]. In a perfectly axisymmetric mirror field, each guiding center moves on its mean magnetic surface, and flux tube cross sections are circular. Very high mirror ratios can be reached in axisymmetric systems. Stability of the flute mode is a main threat in axisymmetric mirrors. The stabilization mechanism in GDT relies on a plasma flow to the expander regions beyond the confinement region. An achievement is that stabilization effects from an expanding flux tube has been demonstrated in GDT, but in certain parameter regimes, the flute mode may not be stable. Improved confinement has then been arranged with a shear poloidal plasma rotation produced by biased potential plates. In such cases, it is envisioned that the sheared rotation cuts large plasma displacements structures into smaller structures near the radius where the plasma rotates in opposite directions [12]. The shear layer may then act as a kind of 'internal transport barrier', but the confinement quality may not be adequate in such scenarios. The shear rotation mechanism does not provide flute stability; rather confinement is rescued to some degree by 'brutally chopping' the large unstable displacements into smaller pieces. A more quiescent confinement would require stability of the flute mode [5].

The study in this paper is on mirrors with a stabilizing quadrupolar field. In a minimum B field created by a quadrupolar field component, the magnetic field strength increases in radial directions away from the magnetic axis [16]. A flux surface in a minimum B field region has concave (or favorable) curvature. Minimum B fields have for a long time been known to be capable of stabilizing the flute mode, and the first experimental report of the dramatic stabilizing effect was published in a classical paper [14]. A drawback of mirrors stabilized by a quadrupolar field is that the ellipticity of the cross sections of the magnetic flux tubes increases with the magnetic field strengths along the axis [9]. The ellipticity needs to be kept within a tolerable range, while flute mode stability should be maintained at the same time. One motivation for the SFLM field with its straight non-parallel field lines is that it may correspond to a minimal ellipticity for a given mirror ratio of a minimum B mirror field [7].

Heating of a plasma in a SFLM device could be carried out with ion cyclotron resonance heating (ICRH), with separate antennas placed near the field maxima on opposite sides of the mid-plane [17, 18]. One antenna system would be used for heating deuterium ions, while the other antenna system on the opposite side of the mid plane would be used for triton heating [17, 18]. The geometry of the SFLM is predicted to enable good antenna coupling and effective plasma heating, where steady state heating is facilitated by the choice of ICRH for the heating [17]. Selecting ICRH frequencies to match resonances at higher field strengths than at the mid plane could reduce power demands and produce a sloshing ion distribution, which could provide a warm plasma stabilization in between the sloshing ion peaks. A scenario is to counteract diffusion into the loss cone by sweeping ICRH frequencies, with a goal to reach a higher fusion Q factor [18]. There is also an option for additional ECRH [19], where a minimum B field corresponds to an attractor state for the ECR waves [19].

Mirror machines, where longitudinal loss from pitch angle scattering and the comparatively low electron temperature pose challenges, have not been developed to a level with adequate confinement for a stand-alone fusion reactor. Confinement demands are much less restrictive in a fusion-fission hybrid reactor scenario [20, 21]. Studies have predicted that a power amplification by fission could be as high as 150 in a mirror hybrid reactor, with reactor safety parameters maintained within safety margins [20], It could then be sufficient with a fusion power of only 10 MW and a fusion Q factor as low as only 0.15 for efficient power production [21], which may be achieved with an electron temperature in the range of only 1 keV. Recent years achievements in mirror experiments indicate that power production from a mirror hybrid reactor is a realistic option. Some of the engineering flexibilities with an open geometry, with a need for a large expander area for a 'divertor system', are indicated in figure 3, and these may turn out to be a crucial advantage for the development of a useful mirror reactor concept.

2. Gyro center motion in a vacuum magnetic field

Let us describe the magnetic field $\mathbf{B} = \nabla W$ in a vacuum region in terms of the scalar magnetic potential W and Clebsch coordinates $x_0(\mathbf{x})$ and $y_0(\mathbf{x})$, and use the curvilinear set (x_0, y_0, W) to describe the guiding center motion. The coordinates are related by

$$B_0 \nabla x_0 \times \nabla y_0 = \nabla W.$$

With B_0 constant, this implies $\nabla^2 W = 0$ and $\nabla \times (\nabla x_0 \times \nabla y_0) = 0$. Furthermore, the orthogonal relations $\nabla W \cdot \nabla x_0 = 0$ and $\nabla W \cdot \nabla y_0 = 0$ imply that the Clebsch coordinates are constant along magnetic field lines. A motivation to use Clebsch coordinates is that the guiding center values of the Clebsch coordinates are slowly varying when the gyro center drifts are small.

The guiding center velocity is written as $\mathbf{v}_{\rm gc} = \mathbf{v}_{\perp,\rm gc} + \mathrm{v}_{\parallel}\hat{\mathbf{B}}$, where the perpendicular drift is given by the standard expression in a vacuum magnetic field:

$$\mathbf{v}_{\perp,\rm gc} = \frac{\mathbf{E} \times \mathbf{B}}{B^2} + \frac{\mu B + m\mathrm{v}_{\parallel}^2}{q} \frac{\mathbf{B} \times \nabla B}{B^3}.$$

Here, all quantities are evaluated at the guiding center position and $\mu = m\mathrm{v}_{\perp}^2/(2B)$ is the magnetic moment adiabatic invariant. The energy conservation of the guiding centers in a stationary field reads

$$\varepsilon = \frac{m\mathrm{v}_{\parallel}^2}{2} + U = \mathrm{const},$$

where $\mathbf{E} = -\nabla\phi$ and $U = \mu B + q\phi$ is the guiding center potential. Using $\dot{\bar{W}} = \mathbf{v}_{\rm gc} \cdot \nabla W$, $\dot{\bar{x}}_0 = \mathbf{v}_{\rm gc} \cdot \nabla x_0$ and $\dot{\bar{y}}_0 = \mathbf{v}_{\rm gc} \cdot \nabla y_0$ for the evolution of the guiding center coordinates, where bars indicate gyro center values, we obtain $\dot{\bar{W}} = B\mathrm{v}_{\parallel}$ and

$$\dot{\bar{x}}_0 = -\frac{1}{B_0}\left(\frac{\partial\phi}{\partial y_0} + \frac{\mu B + m\mathrm{v}_{\parallel}^2}{qB}\frac{\partial B}{\partial y_0}\right), \tag{1a}$$

$$\dot{\bar{y}}_0 = \frac{1}{B_0}\left(\frac{\partial\phi}{\partial x_0} + \frac{\mu B + m\mathrm{v}_{\parallel}^2}{qB}\frac{\partial B}{\partial x_0}\right). \tag{1b}$$

We will here determine the Cartesian-like Clebsch coordinates by choosing the conditions $x_0(\mathbf{x}) \to x$ and $y_0(\mathbf{x}) \to y$ as $\mathbf{x} \to 0$. In cylindrical Clebsch coordinates, defined by the substitutions $x_0 = r_0 \cos\theta_0$ and $y_0 = r_0 \sin\theta_0$, the 'poloidal' and radial drifts can be determined from

$$\bar{r}_0\dot{\bar{\theta}}_0 = \frac{1}{B_0}\left(\frac{\partial\phi}{\partial r_0} + \frac{\mu B + m\mathrm{v}_{\parallel}^2}{qB}\frac{\partial B}{\partial r_0}\right), \tag{1c}$$

$$\dot{\bar{r}}_0 = -\frac{1}{B_0}\left(\frac{1}{r_0}\frac{\partial\phi}{\partial\theta_0} + \frac{\mu B + m\mathrm{v}_{\parallel}^2}{qB}\frac{1}{r_0}\frac{\partial B}{\partial\theta_0}\right). \tag{1d}$$

The last term corresponds to the magnetic drift in the radial direction. As seen, this radial magnetic drift would be zero if the magnetic field strength in the (r_0, θ_0, W) coordinates could be written in the form $B = B(r_0, W)$, which then corresponds to a guiding center motion along a single magnetic surface (local omnigenuity) if the electric potential is independent of θ_0. It needs to be emphasized here that a case with $\partial B/\partial\theta_0 = 0$ is approached not only by axisymmetric mirrors; the criterion is also met, to leading order in the long-thin expansion, by a certain class of quadrupolar mirror magnetic fields [1–3, 7, 22, 23]. Equation (1d) shows that a radial constant of motion, i.e. the guiding center radial coordinate $\bar{r}_0$, can be identified in such a case. The radial invariant can also be extended to situations where the gyro center makes *oscillatory* drift excursions from the mean magnetic surface, but means to ensure the radial confinement has first to be arranged to assure the existence of this invariant. In situations with unbounded radial motions in the collision free approximation, the radial invariant ceases to exist. The point with the radial invariant for a confinement scheme is that it should imply a bounded radial motion in the collision free idealization.

Quasi-neutrality imposes restrictions on possible potential variations in a plasma. In cases where ε, μ, $\bar{r}_0$ are useful constants of motions, the Vlasov treatment in section 6 leads to a quasi-neutral potential in the form $\hat{\phi}(r_0, B)$. The drift equations then become, if the plasma β is neglected:

$$\dot{\bar{x}}_0 = \omega_2 \bar{y}_0, \tag{1e}$$

$$\dot{\bar{y}}_0 = -\omega_1 \bar{x}_0, \tag{1f}$$

$$\omega_1 = -\frac{1}{B_0}\left[\frac{1}{r_0}\frac{\partial\hat{\phi}}{\partial r_0} + \frac{1}{q}\left(\frac{\partial\hat{U}}{\partial B} + \frac{m\mathrm{v}_\parallel^2}{B}\right)\frac{1}{x_0}\frac{\partial B}{\partial x_0}\right]$$

$$\omega_2 = -\frac{1}{B_0}\left[\frac{1}{r_0}\frac{\partial\hat{\phi}}{\partial r_0} + \frac{1}{q}\left(\frac{\partial\hat{U}}{\partial B} + \frac{m\mathrm{v}_\parallel^2}{B}\right)\frac{1}{y_0}\frac{\partial B}{\partial y_0}\right].$$

Here, $\hat{U}(r_0, B) = q\hat{\phi} + \mu B$. We will put special attention to cases where $\omega_1/\omega_2 \approx 1$ in the central confinement region. To see the conditions for this, we observe that

$$\omega_2 = \omega_1 - \frac{1}{qB_0}\left(\frac{\partial\hat{U}}{\partial B} + \frac{m\mathrm{v}_\parallel^2}{B}\right)\frac{1}{x_0 y_0}\frac{\partial B}{\partial\theta_0}. \tag{1g}$$

If $\partial B/\partial\theta_0 = 0$, we obtain $\omega_1 = \omega_2$ and then $\bar{r}_0$ is constant from equations (1e), (1f). Equation (1g) shows that the deviation $\omega_2 - \omega_1$, which produces radial excursions from the mean magnetic surface of a particle, vanishes when the radial magnetic drift is zero, and magnetic shaping is therefore crucial for the possibility to find an arrangement with small radial excursions. For more general quadrupolar mirror fields, a radial electric field can assist in making the ratio ω_1/ω_2 close to unity and slowly varying, where voltage demands are particularly small for a region where the magnetic drift is weak (i.e. the SFLM field), as described in [5]. The WKB solution in [5] then leads to a radial invariant I_r in the form

$$I_r = \sqrt{\left(\frac{\omega_1}{\omega_2}\right)^{1/2}\bar{x}_0^2 + \left(\frac{\omega_2}{\omega_1}\right)^{1/2}\bar{y}_0^2} \approx \bar{r}_0 + \frac{\omega_2-\omega_1}{4\omega_1}\frac{\bar{y}_0^2-\bar{x}_0^2}{\bar{r}_0}.$$

The constant I_r describes a radially bounded gyro center motion in the vicinity of a mean magnetic surface. The size of the radial gyro center excursions $\Delta\bar{r}_0 \equiv \bar{r}_0 - I_r$ can be estimated by

$$\Delta\bar{r}_0 = \frac{\dfrac{\partial\hat{U}}{\partial B} + \dfrac{mv_\parallel^2}{B}}{4qB_0\omega_1}\frac{y_0^2 - x_0^2}{r_0}\left(\frac{1}{y_0}\frac{\partial B}{\partial y_0} - \frac{1}{x_0}\frac{\partial B}{\partial x_0}\right).$$

Since $B(x_0, y_0, W)$ for a quadrupolar mirror field depends on the squares x_0^2 and y_0^2, the displacement $\Delta\bar{r}_0$ is zero along curves $y_0 = \pm x_0$ [5]. With a parabolic electric potential $\hat{\phi} = \hat{\phi}_0 \cdot (r_0^2/a^2)$, we obtain the estimate

$$\frac{|\Delta\bar{r}_0|}{\bar{r}_0} \leqslant \frac{1}{8}\frac{k_B T}{|q\phi_0|}\left|\frac{1}{B}\frac{\partial B}{\partial\theta_0}\right|.$$

With a moderate strength of the radial potential variations ($|q\phi_0| < k_B T$), this predicts substantial radial excursions in a transition region where $\partial B/\partial\theta_0$ is not small. The radial gyro center displacements may for a class of orbits even be larger than the vacuum chamber radius, and radial loss due to collisions is enhanced when $\Delta\bar{r}_0$ is increased. The confinement is better for particles with orbits confined to regions where $\partial B/\partial\theta_0$ is small and the gyro centers move close their mean magnetic surface, whereby neoclassical effect can be neglected. The ratio of the rate of neoclassical to diffusive omnigenous collisional loss can be estimating the squares of the radial displacements in collision events. Therefore, a large value of the ratio

$$\frac{|\Delta\bar{r}_0|^2}{r_g^2},$$

where r_g is the thermal gyro radius, indicates a faster radial loss in regions where $\Delta\bar{r}_0$ is large, with a tendency for a lowered plasma density in those regions. However, neoclassical effects can to a large extent be avoided with appropriate magnetic field designs for quadrupolar mirrors. We need to emphasize that large values of $\Delta\bar{r}_0$ would not appear in regions where $\partial B/\partial\theta_0$ is sufficiently small, and in the paraxial approximation, it is even possible to completely eliminate such regions with appropriate choices of magnetic field (see appendix D for detailed derivation; beneficial orbit effects on Yushmanov ions from a radial electric field is also described in that appendix). The transition region with strong neoclassical effects can therefore be avoided near the axis, but neoclassical effects can become more important in some annular transition region further away from the axis, as indicated in figure 1.

We envision a high density central confinement region where both the mirror effect and small magnitudes of $\Delta\bar{r}_0$ combine for a high quality confinement, followed by a (possibly annular) transition region with larger magnitude of $\partial B/\partial\theta_0$ (and a decreasing density along the longitudinal direction) extending to a surface with maximal strength of B. In the flux expanding region beyond this region, the mirror effect no longer provides confinement, and the plasma density falls to much lower values compared to the central confinement region.

A weak radial electric field may be a tool to make particle orbits radially bounded, at least in the major part of the confinement region. Although there exists regions where the electric field ceases to be effective, the electric drift constrained by quasi neutrality may nevertheless often be expected to improve overall confinement and reduce radial excursions caused by magnetic radial drifts. A radial electric field may even be capable of restoring radial confinement in situations where the radial magnetic drift, in the absence of the counteracting electric drifts, would correspond to an unbounded radial motion in the collision free approximation, compare [1, 3, 5, 22, 24]. The confinement improvement with a slow plasma rotation can be dramatic, even for modest strengths of the radial electric field. This favorable effect is more pronounced in magnetic field regions with slow magnetic drifts [5], and we will here analyze a field configuration with minimal requirements on the electric field strength.

3. A quadrupolar mirror magnetic field with minimal radial drifts

Our aim is to determine a magnetic field with favorable guiding center drift properties. A case where analytical treatments are tractable to identify magnetic field properties is a long-thin approximation. We here consider a long-thin quadrupolar expansion of the scalar magnetic vacuum potential to a higher order than typically done, compare, [1, 2, 5, 9];

$$W = \tilde{W}(z) + \frac{x^2}{2}A_1(z) + \frac{y^2}{2}A_2(z) + x^4\eta_1(z) + x^2y^2\bar{\eta}(z) + y^4\eta_2(z) + \mathrm{O}(\lambda^6), \quad (2a)$$

where $\mathbf{B}_\mathrm{v} = \nabla W$, $\tilde{W}(z) = \int_0^z \mathrm{d}z\tilde{B}(z)$, $\hat{\mathbf{z}}$ is a unit vector along the axis of the long-thin quadrupolar magnetic flux tube, $\hat{\mathbf{z}}\tilde{B}(z)$ is the field on axis, $\nabla \cdot \mathbf{B}_\mathrm{v} = 0$ yields $\nabla^2 W = 0$ and

$$A_1(z) + A_2(z) = -\frac{\mathrm{d}\tilde{B}}{\mathrm{d}z}, \quad (2b)$$

$$\frac{1}{2}A_i'' + 12\eta_i + 2\bar{\eta} = 0, \quad i = 1,\ 2, \quad (2c)$$

where primes denote differentiation with respect to z. The magnetic field components are

$$B_x = x \cdot (A_1 + 4x^2\eta_1 + 2y^2\bar{\eta}), \quad (2d)$$

$$B_y = y \cdot (A_2 + 4y^2\eta_2 + 2x^2\bar{\eta}), \quad (2e)$$

$$B_z = \tilde{B} + \frac{x^2}{2}A_1' + \frac{y^2}{2}A_2' + x^4\eta_1' + x^2y^2\bar{\eta}' + y^4\eta_2'. \quad (2f)$$

The special case of axisymmetric fields corresponds to $A_2 = A_1$ and $\eta_2 = \bar{\eta}/2 = \eta_1$. The focus in this paper is on mirrors with a stabilizing quadrupolar field. We need the magnetic field strength to calculate guiding center drifts:

$$B = \tilde{B} + \frac{x^2}{2}\left(A_1' + \frac{A_1^2}{\tilde{B}}\right) + \frac{y^2}{2}\left(A_2' + \frac{A_2^2}{\tilde{B}}\right) + B^{(2)}, \quad (2g)$$

$$B^{(2)} = x^4P_1 + x^2y^2\overline{P} + y^2P_2, \quad (2h)$$

$$P_i = \eta_i' + 4\frac{A_i}{\tilde{B}}\eta_i - \frac{B}{8}\left(\frac{A_i}{\tilde{B}}\right)^4\left(1+2\frac{\tilde{B}A_i'}{A_i^2}\right), \quad (2i)$$

$$\overline{P} = \bar{\eta}' + 2\frac{(A_1 + A_2)}{\tilde{B}}\bar{\eta} - \frac{\tilde{B}}{4}\left(\frac{A_1A_2}{\tilde{B}^2}\right)^2\left(1 + \frac{\tilde{B}A_1'}{A_1^2} + \frac{\tilde{B}A_2'}{A_2^2}\right). \quad (2j)$$

Each guiding center would move along a single magnetic field line if a vacuum field strength of the form $B = \breve{B}(W)$ could be found, since the magnetic drift vanish for such a configuration. To approach this, we first notice that

$$\breve{B}(W) = \breve{B}(\tilde{W} + W_1) = \breve{B}(\tilde{W}) + W_1 \cdot \frac{\mathrm{d}\breve{B}(\tilde{W})}{\mathrm{d}\tilde{W}} + \frac{W_1^2}{2} \cdot \frac{\mathrm{d}^2\breve{B}(\tilde{W})}{\mathrm{d}\tilde{W}^2} + \ldots..$$

Here, $\breve{B}[\tilde{W}(z)] = \tilde{B}(z)$. The implicit function theorem then implies

$$\frac{\mathrm{d}\breve{B}(\tilde{W})}{\mathrm{d}\tilde{W}} = \frac{1}{\tilde{B}(z)}\frac{\mathrm{d}\tilde{B}}{\mathrm{d}z} \text{ and } \frac{\mathrm{d}^2\breve{B}(\tilde{W})}{\mathrm{d}\tilde{W}^2} = \frac{1}{\tilde{B}}\frac{\mathrm{d}}{\mathrm{d}z}\left(\frac{1}{\tilde{B}}\frac{\mathrm{d}\tilde{B}}{\mathrm{d}z}\right).$$

We thus obtain, including second order terms,

$$B = \breve{B}(W) + B_{\mathrm{rest}},$$

where

$$B_{\mathrm{rest}} = -W_1 \cdot \frac{\tilde{B}'}{\tilde{B}} - \frac{W_1^2}{2} \cdot \frac{1}{\tilde{B}}\frac{\mathrm{d}}{\mathrm{d}z}\left(\frac{1}{\tilde{B}}\frac{\mathrm{d}\tilde{B}}{\mathrm{d}z}\right) + \frac{x^2}{2}\left(A_1' + \frac{A_1^2}{\tilde{B}}\right) + \frac{y^2}{2}\left(A_2' + \frac{A_2^2}{\tilde{B}}\right) + B^{(2)}$$

or

$$B_{\mathrm{rest}} = \frac{x^2}{2}\frac{A_1^2}{\tilde{B}}\left[1 - \frac{\mathrm{d}(\tilde{B}/A_1)}{\mathrm{d}z}\right] + \frac{y^2}{2}\frac{A_2^2}{\tilde{B}} \times \left[1 - \frac{\mathrm{d}(\tilde{B}/A_2)}{\mathrm{d}z}\right] + x^4Q_1 + x^2y^2\bar{Q} + y^4Q_2, \quad (2k)$$

$$Q_1 = \eta_1' + \frac{5A_1 + A_2}{\tilde{B}}\eta_1 - \frac{\tilde{B}}{8}\left(\frac{A_1}{\tilde{B}}\right)^4\left[1 + \frac{2\tilde{B}A_1'}{A_1^2} + \frac{\tilde{B}^2}{A_1^2}\frac{\mathrm{d}}{\mathrm{d}z}\left(\frac{\tilde{B}'}{\tilde{B}}\right)\right],$$

$$Q_2 = \eta_2' + \frac{5A_2 + A_1}{\tilde{B}}\eta_2 - \frac{\tilde{B}}{8}\left(\frac{A_2}{\tilde{B}}\right)^4 \times \left[1 + \frac{2\tilde{B}A_2'}{A_2^2} + \frac{\tilde{B}^2}{A_2^2}\frac{\mathrm{d}}{\mathrm{d}z}\left(\frac{\tilde{B}'}{\tilde{B}}\right)\right],$$

$$\bar{Q} = \tilde{B}^3\frac{\mathrm{d}}{\mathrm{d}z}\left(\frac{\bar{\eta}}{\tilde{B}^3}\right) - \frac{\tilde{B}}{4}\left(\frac{A_1A_2}{\tilde{B}^2}\right)^2 \times \left[1 + \frac{\tilde{B}A_1'}{A_1^2} + \frac{\tilde{B}A_2'}{A_2^2} + \frac{\tilde{B}^2}{A_1A_2}\frac{\mathrm{d}}{\mathrm{d}z}\left(\frac{\tilde{B}'}{\tilde{B}}\right)\right].$$

The magnetic drifts in a vacuum field vanish if B_{rest} would be zero. To leading order, that would be the case if

$$A_1 = \frac{\tilde{B}(z)}{c_1 + z}, \quad (3a)$$

$$A_2 = \frac{\tilde{B}(z)}{c_2 + z} \quad (3b)$$

and equation (2b) gives $\tilde{B}(z) = \frac{B_0c_1c_2}{(c_1+z)(c_2+z)}$, where c_1, c_2 and B_0 are constants. The choice $c_1 = -c_2 = c > 0$ implies

$$\tilde{B}(z) = \frac{B_0}{1 - z^2/c^2}, \quad (3c)$$

which corresponds to a mirror field (the SFLM field) with a field minimum at $z = 0$. The field strength is finite for $|z| < c$, which represents the mirror confined region. The scalar magnetic potential at the z axis become

$$\tilde{W}(z) = cB_0 \ln\sqrt{\frac{c+z}{c-z}}$$

which has the inverse $z/c = \tanh[\tilde{W}/(cB_0)]$. We can then make the identification

$$\breve{B}(W) = B_0 \cosh^2\left(\frac{W}{cB_0}\right).$$

To simplify formula writings, we introduce

$$T_{1,2} = c_{1,2} + z \tag{3d}$$

and obtain by substituting equations (3a), (3b):

$$Q_1 = \frac{1}{T_1^5 T_2}\left\{\frac{\mathrm{d}(T_1^5 T_2 \eta_1)}{\mathrm{d}z} + \left[\frac{3}{8} - \frac{1}{8}\frac{(\Delta c)^2}{T_2^2}\right] B_0 c_1 c_2\right\},$$

$$Q_2 = \frac{1}{T_1 T_2^5}\left\{\frac{\mathrm{d}(T_1 T_2^5 \eta_2)}{\mathrm{d}z} + \left[\frac{3}{8} - \frac{1}{8}\frac{(\Delta c)^2}{T_1^2}\right] B_0 c_1 c_2\right\}.$$

Here, $\Delta c = c_1 - c_2$. We now use equation (2c) and substitute

$$\eta_1 = -\frac{\bar{\eta}}{6} - \frac{B_0 c_1 c_2}{24}\frac{\mathrm{d}^2}{\mathrm{d}z^2}\left(\frac{1}{T_1^2 T_2}\right), \tag{3e}$$

$$\eta_2 = -\frac{\bar{\eta}}{6} - \frac{B_0 c_1 c_2}{24}\frac{\mathrm{d}^2}{\mathrm{d}z^2}\left(\frac{1}{T_1 T_2^2}\right)\Bigg] \tag{3f}$$

to show that $\bar{\eta}(z)$ is a generator for the solutions of $Q_1(z)$, $Q_2(z)$ and $\bar{Q}(z)$:

$$Q_1 = \frac{1}{T_1^5 T_2}\left\{\frac{-1}{6}\frac{\mathrm{d}(T_1^5 T_2 \bar{\eta})}{\mathrm{d}z}\left[-\frac{3}{4} + \frac{7}{4}\left(\frac{\Delta c}{T_2}\right)^2 + \left(\frac{\Delta c}{T_2}\right)^3\right]\frac{B_0 c_1 c_2}{6}\right\},$$

$$Q_2 = \frac{1}{T_1 T_2^5}\left\{\frac{-1}{6}\frac{\mathrm{d}(T_1 T_2^5 \bar{\eta})}{\mathrm{d}z} + \left[-\frac{3}{4} + \frac{7}{4}\left(\frac{\Delta c}{T_1}\right)^2 - \left(\frac{\Delta c}{T_1}\right)^3\right]\frac{B_0 c_1 c_2}{6}\right\},$$

$$\bar{Q} = \frac{1}{T_1^3 T_2^3}\left[\frac{\mathrm{d}(T_1^3 T_2^3 \bar{\eta})}{\mathrm{d}z} + \frac{3}{4} B_0 c_1 c_2\right].$$

In a system without magnetic drift all the three quantities $Q_1(z)$, $Q_2(z)$ and $\bar{Q}(z)$ have to be zero, but it is evident that this is not possible. Magnetic drifts are thus unavoidable in the higher order long-thin expansion for the quadrupolar mirror field, although disappearance of the magnetic drifts can be arranged for the leading terms in the expansion. To higher order in the expansion, the best we may hope for is an omnigenous equilibrium, where each guiding center moves on a single magnetic surface, instead of a motion on a single magnetic field line. Even this turns out to be impossible in our case. Oscillatory guiding center excursions from the magnetic surface would be tolerable, and there is confidence that this can be arranged with a weak radial electric field for a central confinement region. The aim in this study is to identify a suitable magnetic mirror field to the considered higher order long-thin expansion. This can enable designs of more compact 'short-fat' mirror configurations with favorable radial confinement. In addition, average minimum B properties for gross plasma stability is achieved to leading order [7].

In our case, it is sufficient to consider leading order expressions for the Clebsch coordinates:

$$x_0(\mathbf{x}) = \frac{x}{1 + \gamma_1(z)} + O(\lambda^3), \tag{4a}$$

$$y_0(\mathbf{x}) = \frac{y}{1 + \gamma_2(z)} + O(\lambda^3). \tag{4b}$$

A check show that

$$\frac{\gamma'_i}{1 + \gamma_i(z)} = \frac{A_i}{\tilde{B}}, \quad i = 1,\ 2. \tag{4c}$$

We are free to choose $\gamma_i(0) = 0$ at the mid-plane $z = 0$, and near the axis and close to the mid-plane the expressions thus approach $x_0(\mathbf{x}) \to x$ and $y_0(\mathbf{x}) \to y$. Equations (3a), (3b) and (4c) then gives the leading order expressions

$$x_0(\mathbf{x}) = \frac{x}{1 + z/c_1} + O(\lambda^3), \tag{4d}$$

$$y_0(\mathbf{x}) = \frac{y}{1 + z/c_2} + O(\lambda^3). \tag{4e}$$

The case $c_1 = -c_2 = c > 0$ corresponds to a mirror field (the SFLM field) with straight non-parallel magnetic field lines near the axis, where the magnetic field lines are parametrized as $x(z) = (1 + z/c)x_0$ and $y(z) = (1 - z/c)y_0$. A flux surface with constant r_0 has elliptical cross section near the axis

$$r_0^2 = \left(\frac{x}{1 + z/c}\right)^2 + \left(\frac{y}{1 - z/c}\right)^2.$$

The 'ellipticity' (eccentricity or aspect ratio) is in this case given by

$$\varepsilon_{\mathrm{ell}}(z) = \frac{1 + |z|/c}{1 - |z|/c} = [\sqrt{R_m} + \sqrt{R_m - 1}]^2.$$

Here, $R_m(z) = \tilde{B}/B_0$ is the mirror ratio along the axis. These elliptical cross sections degenerate into curves (or infinitely thin ellipses) at the focal lines $z = \pm c$ where the magnetic field becomes infinite. The confinement region is a finite field region with a finite mirror ratio (a mirror ratio in the range 4–6 is representative and may provide a tolerable ellipticity). For a given finite maximal value of a mirror ratio, the SFLM could have minimal ellipticity properties for a minimum B stabilized quadrupolar field, since it is to leading order a marginal minimum B field, and a mirror ratio of 4 corresponds to an ellipticity of only 13.9. Considerably higher ellipticities can appear in mirror machines which have differently shaped quadrupolar fields for the MHD stabilization purpose. The flux tube has the characteristic quadrupolar shape, where identical fields (in a non-disturbed case) are obtained on opposite sides of the mid-plane after a 90° rotation around the z axis. Numerical modeling of 3D coils predict that compact superconducting coils can be designed to create the field in the confinement region [25], with sufficient space available for a reactor blanket region in between the coils and the vacuum chamber containing the plasma, see figure 3. The aim of the quadrupolar magnetic field is to appproach an average minimum B field for stability of the flute mode. The striking stabilization effect has since its introduction in the 1960s been confirmed in numerous experiments at different laboratories.

Returning to the magnetic field strength, we find with $A_1 = \frac{B_0 c_1 c_2}{T_1^2 T_2}$ and $A_2 = \frac{B_0 c_1 c_2}{T_1 T_2^2}$:

$$B_{\text{rest}} = x_0^4 S_1(z) + x_0^2 y_0^2 \bar{S}(z) + y_0^4 S_2(z) + O(\lambda^6).$$

Here, with $K = B_0 c_1 c_2$, $S_1 = \left(\frac{T_1}{c_1}\right)^4 Q_1$, $S_2 = \left(\frac{T_2}{c_2}\right)^4 Q_2$ and $\bar{S} = \left(\frac{T_1}{c_1}\right)^2 \left(\frac{T_2}{c_2}\right)^2 \bar{Q}$;

$$S_1(z) = \frac{1}{6c_1^4} \frac{1}{T_1 T_2} \left\{ -\frac{\mathrm{d}}{\mathrm{d}z}\left(\frac{T_1^2}{T_2^2}\eta\right) + K \cdot \left[-\frac{3}{4} + \frac{7}{4}\left(\frac{\Delta c}{T_2}\right)^2 + \left(\frac{\Delta c}{T_2}\right)^3 \right] \right\}, \tag{5a}$$

$$S_2(z) = \frac{1}{6c_2^4} \frac{1}{T_1 T_2} \left\{ -\frac{\mathrm{d}}{\mathrm{d}z}\left(\frac{T_2^2}{T_1^2}\eta\right) + K \cdot \left[-\frac{3}{4} + \frac{7}{4}\left(\frac{\Delta c}{T_1}\right)^2 - \left(\frac{\Delta c}{T_1}\right)^3 \right] \right\}, \tag{5b}$$

$$\bar{S}(z) = \frac{1}{c_1^2 c_2^2} \frac{1}{T_1 T_2} \left(\frac{\mathrm{d}\eta}{\mathrm{d}z} + \frac{3}{4}K \right), \tag{5c}$$

where we have substituted

$$\eta(z) = (T_1 T_2)^3 \bar{\eta}. \tag{5d}$$

With $x_0 = r_0 \cos\theta_0$ and $y_0 = r_0 \sin\theta_0$, we find from standard trigonometric relations

$$B_{\text{rest}}(r_0, \theta_0, W) = r_0^4 \cdot \left[\frac{3(S_1 + S_2) + \bar{S}}{8} + \frac{S_1 - S_2}{2} \times \cos 2\theta_0 + \frac{S_1 + S_2 - \bar{S}}{8} \cos 4\theta_0 \right]. \tag{5e}$$

To leading order z is a function only of W, i.e. $z/c = \tanh[\tilde{W}/(cB_0)]$. The quantities S_1, S_2, $\bar{S}$ appearing in the expression for $B_{\text{rest}}(r_0, \theta_0, W)$ are therefore functions of W, and radial drifts are associated with the dependence of $B(r_0, \theta_0, W)$ on the Clebsch angle θ_0. The $\cos 2\theta_0$ dependence is eliminated if $S_2 = S_1$, while the $\cos 4\theta_0$ dependence is eliminated if $\bar{S} = S_1 + S_2$. Equations (5a)–(5c) prohibit that both of these equations are satisfied simultaneously: In the case $c_1 = -c_2 = c > 0$, equations (5a)–(5c) can with

$$\tilde{c}^2 = c^2 - z^2 \tag{6}$$

be written (see appendix A for derivation)

$$6S_1 = H_0 + \frac{1}{c^4 \tilde{c}^2} \frac{\mathrm{d}}{\mathrm{d}z} \left[\frac{T_1^2}{T_2^2}(\eta - \eta_0) \right], \tag{7a}$$

$$6S_2 = H_0 + \frac{1}{c^4 \tilde{c}^2} \frac{\mathrm{d}}{\mathrm{d}z} \left[\frac{T_2^2}{T_1^2}(\eta - \eta_0) \right], \tag{7b}$$

$$\bar{S} = H_0 - \frac{1}{c^4 \tilde{c}^2} \frac{\mathrm{d}(\eta - \eta_0)}{\mathrm{d}z}, \tag{7c}$$

where

$$\eta_0(z) = B_0 c^3 \left(\frac{3}{4} + \frac{1}{2} \frac{c^2}{c^2 + z^2} \right) \cdot \frac{z}{c}, \tag{7d}$$

$$H_0(z) = -\frac{1}{2} \frac{B_0}{c^4} \left(\frac{c^2}{c^2 + z^2} \right)^2. \tag{7e}$$

A choice to keep the radial drift small is $S_2 = S_1$. That case corresponds to $\eta = \eta_0$ and $\bar{S} = S_1/6 = S_2/6 = H_0(z)$. We then find

$$B_{\text{rest}}(r_0, \theta_0, W) = -\frac{B_0}{8} \left(\frac{c^2}{c^2 + z^2} \right)^2 \cdot \frac{r_0^4}{c^4} \left(1 - \frac{\cos 4\theta_0}{3} \right) = -\frac{B_0}{8} \left(\frac{1}{1 + \tanh^2 \bar{W}} \right)^2 \cdot \frac{r_0^4}{c^4} \left(1 - \frac{\cos 4\theta_0}{3} \right), \tag{8a}$$

where $\overline{W} = W/(cB_0)$. Thus $\partial B/\partial\theta_0$ is finite, and therefore a radial magnetic drift is present, although we have eliminated the drift associated with the term $\cos 2\theta_0$. The function $c^4/(c^2 + z^2)^2$ decreases slowly from unity at the mid-plane and approaches ¼ as $z \to \pm c$. The magnetic radial drift effects are therefore somewhat weaker away from the mid-plane for this magnetic field. The radial component of the magnetic drift,

$$\frac{\mathrm{d}\bar{r}_0}{\mathrm{d}t} = \frac{1}{8} \frac{\mu\bar{B} + m\bar{v}_\parallel^2}{q\bar{B}} \left(\frac{c^2}{c^2 + \bar{z}^2} \right)^2 \cdot \frac{\bar{r}_0^3}{c^4} \frac{4 \sin 4\bar{\theta}_0}{3} \tag{8b}$$

is zero for the angles $\bar{\theta}_0 = p\pi/4$, where p is an integer and bars are used here to denote gyro center values. At a first glance, the worst added radial drifts may be expected for 'sector locked' particles, i.e. particles locked into angle sectors in between the values $\bar{\theta}_0 = p\pi/4$, while a tendency for cancellation of the radial excursions is expected for particles that encircle the axis (in passing, this view is also in line with a corresponding cancellation tendency provided if a radial electric field would be added). However, the lowest order drifts near the axis approach zero for this field (each gyro center moves along a single magnetic field line to leading order), and it is therefore not immediately clear whether or not particles encircle the axis in the higher order solution. In fact, the poloidal magnetic drift component for this field

$$\bar{r}_0 \frac{\mathrm{d}\bar{\theta}_0}{\mathrm{d}t} = -\frac{1}{8} \frac{\mu\bar{B} + m\bar{v}_\parallel^2}{q\bar{B}} \left(\frac{c^2}{c^2 + \bar{z}^2} \right)^2 \cdot \frac{4\bar{r}_0^3}{c^4} \left(1 - \frac{\cos 4\bar{\theta}_0}{3} \right) \tag{8c}$$

has a definite sign, and all gyro centers encircle the axis in opposite directions for charges with opposite signs. No particles are sector locked, and the cancellation tendency acts on all particles. This is more transparent by noticing that the drift equations in this field for all particles have the first integral

$$\tilde{I}_r = \bar{r}_0 \cdot \left(1 - \frac{\cos 4\bar{\theta}_0}{3} \right)^{1/4} = \text{const.} \tag{9a}$$

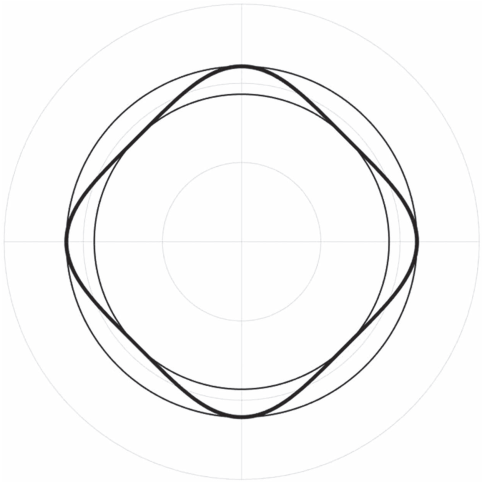

Figure 4. Contour in the mid-plane of a curve $r_0 = \tilde{I}_r \cdot \left(1 - \frac{\cos 4\theta_0}{3}\right)^{-1/4}$, where $\tilde{I}_r$ is constant. The projection of the drift surface has this shape for all particles when only the vacuum magnetic field contributes to the drift. At the mid-plane, the flux surface cross sections have a circular shape, and the figure illustrates how the drift motion is bounded into a region between two flux surfaces. The radial excursion from the mean flux surface could be reduced to almost zero by adding a weak radial electric field.

This ensures a bounded radial motion. The first integral corresponds to an intersection of regions with constant B and regions with constant W, and the guiding centers move along trajectories with the constancy of $\tilde{I}_r$ intact. The constant $\tilde{I}_r$ corresponds to a mean drift surface of the particle motion (projected on a surface $W=$ constant), where radial excursion excursions from the mean magnetic surface are determined by equation (9a). Although the constant $\tilde{I}_r$ ensures a bounded radial motion, the radial drift in this magnetic field accumulate a moderate radial excursion from the mean flux surface (the poloidal magnetic drift is too slow to provide a fast distinct cancellation). The radial excursions are bounded by

$$\left(\frac{3}{4}\right)^{1/4} \leqslant \frac{\bar{r}_0}{\tilde{I}_r} \leqslant \left(\frac{3}{2}\right)^{1/4} \tag{9b}$$

or approximately $0.93 < \bar{r}_0/\tilde{I}_r < 1.11$, which roughly is a 20% relative spread of the radial coordinate along the gyro center trajectory. These radial excursions are illustrated in figure 4. Reduction of the radial excursions to much smaller values is expected if a radial electric field is added, where the $(\mathbf{E}\times\mathbf{B})/B^2$ velocity needs to be somewhat faster than the slow poloidal magnetic drift to be efficient. For this particular field, the voltage demands would be exceptionally small to produce such a radial electric field. In Cartesian coordinates, the first integral can be written

$$\tilde{I}_r = \left\{\frac{2}{3}\left[\left(\frac{x}{c+z}\right)^4 + \left(\frac{y}{c-z}\right)^4 + 6\left(\frac{x}{c+z}\right)^2\left(\frac{y}{c-z}\right)^2\right]\right\}^{1/4} = \text{const.}$$

A radial magnetic drift thus appear to higher order in the expansion. The particular field considered here gives only a minor radial magnetic drift. This field, which is an extension of the SFLM field to higher order in the long-thin expansion, has properties which seems valuable as a base for a high quality confinement magnetic field, since magnetic drifts are minimized and there is the option to add a controlled radial electric field to achieve ideal radial confinement in the collision free approximation, with each guiding center moving close to a magnetic surface in the central confinement region.

We complete this section by writing down expressions for the magnetic field components;

$$B_x = \frac{x}{c+z}\tilde{B}(z)\cdot(1+\varepsilon_x), \tag{10a}$$

$$B_y = -\frac{y}{c-z}\tilde{B}(z)\cdot(1+\varepsilon_y), \tag{10b}$$

$$B_z = \tilde{B}(z)\cdot(1+\varepsilon_z). \tag{10c}$$

Here,

$$\varepsilon_x = \left[\frac{z}{c-z}\frac{h(z)}{6} - \frac{2}{3}\frac{c^2-2cz+3z^2}{\tilde{c}^2}\right]\frac{x^2}{\tilde{c}^2} - \frac{z}{c-z}\frac{h(z)}{2}\frac{y^2}{\tilde{c}^2}, \tag{10d}$$

$$\varepsilon_y = \frac{z}{c+z}\frac{h(z)}{2}\frac{x^2}{\tilde{c}^2} + \left[-\frac{z}{c+z}\frac{h(z)}{6} - \frac{2}{3}\frac{c^2+2cz+3z^2}{\tilde{c}^2}\right]\frac{y^2}{\tilde{c}^2}, \tag{10e}$$

$$\varepsilon_z = \frac{3z-c}{c+z}\frac{x^2}{2\tilde{c}^2} - \frac{3z+c}{c-z}\frac{y^2}{2\tilde{c}^2} + \mathrm{O}(\lambda^4), \tag{10f}$$

where $h(z) = (5c^2+3z^2)/(c^2+z^2)$ and it is straightforward to calculate ε_z to one order higher. The magnetic field lines are not perfectly straight to the higher order in the expansion. This can be seen from a higher order expression for the Clebsch coordinates (see appendix C for derivation). Explicit formulas are with $\tilde{x}_0 = \frac{cx}{c+z}$ and $\tilde{y}_0 = \frac{cy}{c-z}$:

$$x_0 = \tilde{x}_0\cdot\left\{1 + \frac{\tilde{x}_0^2}{6c^2}\tan^{-1}\left(\frac{z}{c}\right) + \frac{\tilde{y}_0^2}{2c^2}\left[-\frac{c+3z}{c+z} + \tan^{-1}\left(\frac{z}{c}\right)\right]\right\}$$

$$y_0 = \tilde{y}_0\cdot\left\{1 + \frac{\tilde{x}_0^2}{2c^2}\left[-\frac{c-3z}{c-z} - \tan^{-1}\left(\frac{z}{c}\right)\right] - \frac{\tilde{y}_0^2}{6c^2}\tan^{-1}\left(\frac{z}{c}\right)\right\}.$$

From this we observe that the ratio B_y/B_x is not constant along magnetic field lines, i.e. this ratio is not solely a function of the Clebsch coordinates in the higher order solution, and the field lines therefore deviate slightly from straight lines.

The arc length along $\mathbf{B}$, derived in appendix B, is given by the expression

$$s = z + \frac{1}{2}\left(\frac{x^2}{c+z} - \frac{y^2}{c-z}\right) - \frac{z+k_1}{8}\frac{\tilde{x}_0^4}{c^4} - \frac{z+\bar{k}}{4}\frac{\tilde{x}_0^2\tilde{y}_0^2}{c^4} - \frac{z+k_2}{8}\frac{\tilde{y}_0^4}{c^4},$$

where k_1, $\bar{k}$, k_2 are constants. A part from corrections of order λ^6, this formula gives $|\nabla s| = 1 + r_0^4/(4c^4)$, and thus $|\nabla s| > 1$. The leading order terms correspond to $\nabla s \to \hat{\mathbf{B}}$, but we obtain $|\nabla s| > 1$ when higher order terms are included, and ∇s therefore also contains components perpendicular to $\hat{\mathbf{B}}$.

4. Poloidal drift and effects of a radial electric field

The magnetic drift in the poloidal direction given by equation (8c) is incredibly small as a result of the reduction of the drifts in this particular magnetic field. This can be illustrated with a representative parameter case with a particle energy of 20 keV, $\bar{r}_0 = 1$ m, $c = 10$ m, and $B = 1$ T, which gives the astonishingly small estimate

$$\left| \bar{r}_0 \frac{\mathrm{d}\bar{\theta}_0}{\mathrm{d}t} \right|_{\text{magn.drift}} < 1 \text{ m s}^{-1}. \tag{11a}$$

Other effects, such as field errors or radial electric fields, would certainly overrule this velocity even at vanishingly small strengths of those effects. In the vacuum magnetic field considered in this paper, the oscillatory radial magnetic drift has a similar small magnitude as the magnetic drift along the poloidal direction. The property that each guiding center moves along a single magnetic field line is only slightly disturbed in the higher order solution by such a vanishingly small magnetic drift.

In this vacuum magnetic field, the evolution of the gyro center radial coordinate obeys

$$\left(\frac{\mathrm{d}\bar{r}_0}{\mathrm{d}\bar{\theta}_0}\right)_{\text{magn.drift}} = -\frac{\bar{r}_0}{4}\frac{\frac{\mathrm{d}}{\mathrm{d}\bar{\theta}_0}\left(1 - \frac{\cos 4\bar{\theta}_0}{3}\right)}{1 - \frac{\cos 4\bar{\theta}_0}{3}}. \tag{11b}$$

The order of magnitude of the ratio between the changes $\mathrm{d}\bar{r}_0$ and $\mathrm{d}\bar{\theta}_0$, in case that only vacuum magnetic drifts are present, can be estimated from this formula, and the expression for the first integral $\tilde{I}_r$ can be derived. Presence of other poloidal drifts can cause profound modifications in $\mathrm{d}\bar{\theta}_0$ and in the ratio $\mathrm{d}\bar{r}_0/\mathrm{d}\bar{\theta}_0$ and change the situation drastically.

To see this, let us add a radial electric field in the confining region, where we for simplicity assume a quadratic dependence on the flux radius in the plasma confining region:

$$\phi = \phi_0 \frac{r_0^2}{a^2}.$$

Here, the constant ϕ_0 is the electric potential at the plasma boundary $r_0 = a$. With $\mathbf{v}_E = (\mathbf{E} \times \mathbf{B})/B^2$, the ratio

$$\varepsilon_E = \frac{\left(\bar{r}_0 \frac{\mathrm{d}\bar{\theta}_0}{\mathrm{d}t}\right)_{\text{magn.drift}}}{\bar{r}_0 \nabla\bar{\theta}_0 \cdot \mathbf{v}_E} \tag{11c}$$

is small even for modest values of ϕ_0, and the $\mathbf{E} \times \mathbf{B}$ drift becomes the dominant poloidal drift in the considered magnetic field. Even a ϕ_0 as small as a few volt (sign does not matter) would be sufficient to make the $\mathbf{E} \times \mathbf{B}$ drift the dominant poloidal drift in this particular field. If we increase the strength of ϕ_0 to, say ± 200 V, there are also margins to compensate for other disturbances such as field errors in the magnetic field design (for instance, geometrical constraints on the coil design is accompanied with unavoidable field errors which grow if the mirror ratio is increased or the device is shortened). The evolution of the radial gyro center coordinate is with such a radial electric field then determined by

$$\left(\frac{\mathrm{d}\bar{r}_0}{\mathrm{d}\bar{\theta}_0}\right)_{\mathbf{E}\times\mathbf{B}\text{ drift}} \approx -\varepsilon_E \frac{\bar{r}_0}{3}\sin 4\bar{\theta}_0 \approx -\langle\varepsilon_E\rangle_b \frac{\langle\bar{r}_0\rangle_b}{3}\sin 4\bar{\theta}_0, \tag{11d}$$

where $\langle\varepsilon_E\rangle_b$ and $\langle\bar{r}_0\rangle_b$ are longitudinal bounce averages. The corresponding solution

$$\bar{r}_0 = \langle\bar{r}_0\rangle_b \cdot \left(1 + \langle\varepsilon_E\rangle_b \frac{\cos 4\bar{\theta}_0}{12}\right) \tag{11e}$$

reveals that the radial excursions from the mean magnetic surface $\langle\bar{r}_0\rangle_b$ is reduced by a factor $\langle\varepsilon_E\rangle_b$. For moderate values of the potential ϕ_0, this means that the radial excursions can be neglected. We may rephrase this observation by stating that a magnetic field for the central confinement region is identified where *each gyro center moves close to a single magnetic surface with minor deviation.*

5. Minimum *B* properties

Flute mode displacements are large scale 'kink' perturbations of the plasma in mirrors, which need to be controlled. Minimum B, or average minimum B, fields have for a long time been used in mirror experiments to stabilize flute modes. The anchor cells in the Gamma10 tandem mirror have minimum B fields with a strong ellipticity ($\varepsilon_{\text{ell}} \approx 50$). A strict, local minimum B field would satisfy $\partial B/\partial r_0 \geqslant 0$, but an inspection of equation (8a) shows that $\partial B/\partial r_0$ is negative for that field, although the leading terms in the long-thin expansion corresponds to a marginal condition with $\partial B/\partial r_0 = 0$, so the minimum B criterion is only 'mildly violated' by the terms in the higher order expansion. In equation (8a) this is revealed by the smallness of the factor r_0^4/c^4. Other effects, for instance line tying or gas dynamic stabilization, which is a main motivation for the GDT project, may for this reason be capable of stabilizing the flute mode. Wall stabilization could be important, although the effect is somewhat weakened in mirror geometry by the smaller induced wall currents. Shear plasma rotation, associated with a radial electric field changing sign at a specific flux radius, has also been used in mirrors to improve confinement and control the evolvement of flute mode displacements. A robust option could be to strengthen the quadrupolar field near the axis, so that the quadrupolar field corresponds to a field with $\partial B/\partial r_0 > 0$ instead of only a marginal minimum B field for the leading order solution near the axis. Aside from that such a choice would make our analysis more complex, a negative physical aspect is that it would increase the ellipticity of the flux tube cross sections.

We will here continue our study with the SFLM field as the leading order solution, and investigate if other choices for the quantities S_1, S_2, $\overline{S}$ could lead to more favorable minimum B properties (appendix B give a clarification on how the arc length in these equilibria are connected with a common formula). If the resulting flux surfaces would be concave (i.e. favorable) or convex may not be obvious beforehand, since the curvature of the field lines is zero in the leading order SFLM field. We will show that the expansion with the SFLM field as the leading order solution leads to convex flux surfaces. For the analysis, we substitute

$$w_0 = 3(S_1 + S_2) + \overline{S},\ \frac{w_2}{4} = S_1 - S_2,\ w_4 = S_1 + S_2 - \overline{S}.$$

Then $B = \breve{B}(W) + \frac{r_0^4}{8} \cdot (w_0 + w_2 \cos 2\theta_0 + w_4 \cos 4\theta_0)$, and a local minimum B criterion is

$$w_0 + w_2 \cos 2\theta_0 + w_4 \cos 4\theta_0 \geqslant 0. \tag{12a}$$

This inequality would imply $\partial B/\partial r_0 \geqslant 0$ for all Clebsch angles if $w_0 > 0$ and $|w_2| + |w_4| \leqslant w_0$. However, equations (7a)–(7c) imply conditions on w_0, w_2, w_4 which may rule out any possibility to find a minimum B field. Equations (7a)–(7c) yield with $\eta_1 = \eta - \eta_0$

$$w_0 = 2H_0 + \frac{8}{c^4\tilde{c}^2}\frac{\mathrm{d}}{\mathrm{d}z}\left(\frac{c^2z^2}{\tilde{c}^4}\eta_1\right),$$

$$w_2 = \frac{16}{3}\frac{1}{c^4\tilde{c}^2}\frac{\mathrm{d}}{\mathrm{d}z}\left[\frac{(c^2+z^2)cz}{\tilde{c}^4}\eta_1\right],$$

$$w_4 = -\frac{2}{3}H_0 + \frac{4}{3}\frac{1}{c^4\tilde{c}^2}\frac{\mathrm{d}}{\mathrm{d}z}\left(\frac{c^4+z^4}{\tilde{c}^4}\eta_1\right).$$

The equations become more transparent with the substitutions

$$\eta_1 = \frac{B_0}{c}\tilde{c}^4 G(z),\ \bar{z} = z/c,\ \overline{w}_k = \frac{c^4 w_k}{B_0},\ k = 0,\ 2,\ 4.$$

Then

$$\bar{w}_0 = -\frac{1}{(1+\bar{z}^2)^2} + \frac{8}{1-\bar{z}^2}\frac{\mathrm{d}(\bar{z}^2G)}{\mathrm{d}\bar{z}}, \tag{12b}$$

$$\bar{w}_2 = \frac{16/3}{1-\bar{z}^2}\frac{\mathrm{d}[(1+\bar{z}^2)\bar{z}\cdot G]}{\mathrm{d}\bar{z}}, \tag{12c}$$

$$\bar{w}_4 = \frac{1/3}{(1+\bar{z}^2)^2} + \frac{4/3}{1-\bar{z}^2}\frac{\mathrm{d}[(1+\bar{z}^4)G]}{\mathrm{d}\bar{z}}. \tag{12d}$$

The case $G = 0$ is recognized as the solution with $w_2 = 0$. Let us continue with the case $w_4 = 0$, which, with k_4 a constant, yields

$$4G = -\frac{1}{1+\bar{z}^4}\left(\frac{\bar{z}}{1+\bar{z}^2} + k_4\right).$$

However, that gives $w_0 < 0$ near $z = 0$. More generally, we see that the inequality (12a) cannot be satisfied with $w_0 > 0$ near the mid-plane for any choice of G, since with

$$G(z) \to c_k \bar{z}^k,\ \bar{z} \to 0$$

we need $k = -1$ in equation (12b) to obtain $w_0 > 0$, but then w_4 becomes singular near the mid-plane, as seen from equation (12d). We conclude that the inequality (12a) cannot be satisfied in the higher order expansion for any vacuum field where the leading terms correspond to the SFLM field.

The case $w_2 = 0$ has the advantage that the magnetic drifts are exceptionally small and a bounded radial motion for all particles is prescribed by the existence of the invariant $\tilde{I}_r$. Wall stabilization and line tying could be sufficient to stabilize the flute mode. Strengthening the quadrupolar magnetic field near the axis is an additional option.

6. Inclusion of finite β field with use of radial invariant

Determination of contributions from the plasma currents to the magnetic field can conveniently be carried out (to first order in β) with the aid of a radial invariant in solutions of the Vlasov equation, provided the radial magnetic drifts are negligible. It will be seen that the resulting expressions correspond to formulas obtained in a fluid approach with the pressure $P(r_0, B)$ depending on the flux coordinate and the magnetic field modulus. We will also investigate possible space dependencies of the electric potential in the plasma.

We assume arrangement of a confinement field, where the gyro center of each particle is moving close to its mean magnetic surface. We then need to carefully design a confining magnetic field, supported by a proper electric field, to achieve this goal. Such fields are identified here for quadrupolar mirrors. It may be mentioned that in toroidal geometries, it is assumed that a nested flux surface system is arranged. This is a necessary condition for confinement, since the nested flux surfaces are a lowest order approximation for the region where the gyro motion is intended to take place. Nested flux surfaces can be a complex task to arrange for stellarators, and, if field disturbances are included, also a concern for almost axisymmetric tori such as tokamaks. Another obstacle is that existence of nested flux surfaces in stellarators does not guarantee a radially bounded particle motion, and often a given set of nested flux surfaces has poor radial confinement due to radial magnetic drifts. A radial electric field, which may spontaneously be generated from a vanishingly small transient radial loss of charged particles, has theoretically been shown to provide quite a dramatic favorable effect on the confinement in a mirror embedded in a stellarator geometry [24]. Essentially, if flux surfaces exist in a stellarator geometry, confinement for most of the particles may be arranged by the generated radial electric field, but this mechanism is less efficient for particles with higher energies, which are predicted to be lost, despite the action of the spontaneously generated electric field [24]. Although radially bounded orbits could be arranged for a large class of particles in toroidal confinement, it is often inaccurate to state that each gyro center moves close to its mean magnetic surface. Deviations between drift and mean magnetic surface as well as banana widths can be large.

In open mirror geometries, there may be less concerns for radial confinement (the longitudinal loss is usually expected to be a dominant loss channel, but the radial loss may become comparable if gross instabilities or strong radial drifts are not eliminated). The existence of flux surfaces is straightforward in mirrors, but gyro center drifts (due to deviation from axisymmetry) can result in radial loss of particles [5]. A beneficial option in open geometries is the availability to arrange a radial electric field by biased electric potential plates outside the confining region, where the magnetic field lines intersect the plates. The radial electric field and the associated weak poloidal plasma rotation can be controlled by the biased potentials. This beneficial influence of biased plates is predicted to work also on particles with higher energies in mirror devices, but it is essential to keep radial magnetic drifts within a tolerable range.

A configuration is assumed where each guiding center moves close to its mean magnetic surface. In case magnetic drifts would tend to ruin this radial confining property, we may improve the situation by adding a radial electric field. Two standard constants of motion, i.e. the magnetic moment μ and the energy ε of the particles, can be used to describe longitudinal confinement to a region $B < (\varepsilon - q\phi)/\mu \approx \varepsilon/\mu$:

$$\mu(\mathbf{x}, \mathbf{v}) = \frac{mv_\perp^2/2}{B(\mathbf{x})}, \tag{13a}$$

$$\varepsilon(\mathbf{x}, \mathbf{v}) = \frac{m}{2}(v_\parallel^2 + v_\perp^2) + q\phi(\mathbf{x}) = \frac{mv_\parallel^2}{2} + \mu B + q\phi. \tag{13b}$$

If the particles would move close its mean magnetic surface, the gyro center radial Clebsch coordinate $\bar{r}_0(\mathbf{x}, \mathbf{v})$ is a convenient third constant of motion, compare [4, 5]:

$$\bar{r}_0(\mathbf{x}, \mathbf{v}) = r_0 - r_{0,g} \approx \text{const}. \tag{13c}$$

Here, $r_0(\mathbf{x})$ is the radial Clebsch coordinate of the particle and $r_{0,g}(\mathbf{x}, \mathbf{v})$ is the small but fast 'gyro ripple' associated with the gyro oscillations of the particle around the magnetic field:

$$r_{0,g}(\mathbf{x}, \mathbf{v}) = \frac{\bar{x}_0}{\bar{r}_0}\frac{v_\perp}{\Omega}|\nabla\bar{x}_0|\cos(\varphi_g + \alpha) - \frac{\bar{y}_0}{\bar{r}_0}\frac{v_\perp}{\Omega}|\nabla\bar{y}_0|\sin\varphi_g. \tag{13d}$$

Here, $\Omega = qB/m$ is the gyro angular frequency, $\varphi_g = \int_{t_0}^{t} \Omega\, \mathrm{d}t$ is the gyro angle for the gyro motion around the magnetic field lines and $\sin\alpha = \nabla x_0 \cdot \nabla y_0/(|\nabla x_0||\nabla y_0|)$ is finite when ∇x_0 and ∇y_0 are not in perpendicular directions. Existence of a third invariant in this form assures radial confinement (in passing, it can be noticed that constancy of the second adiabatic invariant $J_\parallel$ does not generally imply radial confinement [26]). In a collision free idealization, we therefore consider an equilibrium described by distributions functions of the form

$$f_\alpha(\mathbf{x}, \mathbf{v}) = \overline{F}_\alpha[\varepsilon(\mathbf{x}, \mathbf{v}), \mu(\mathbf{x}, \mathbf{v}), \bar{r}_0(\mathbf{x}, \mathbf{v})]. \tag{14a}$$

The label α is used to distinguish ions and electrons. For small gyro radii, this can be written [4]

$$f_\alpha(\mathbf{x}, \mathbf{v}) = F_\alpha - r_{0,g}\frac{\partial F_\alpha}{\partial r_0}, \tag{14b}$$

where $F_\alpha = \overline{F}_\alpha(\varepsilon, \mu, r_0)$ corresponds to the values at the position of the particle. The particle location is displaced radially from the guiding center by the gyro ripple term $r_{0,g}(\mathbf{x}, \mathbf{v})$. The term F_α contributes to the plasma density and the pressure tensor components, but not to the plasma currents perpendicular to the vacuum magnetic field $\mathbf{B}_\mathrm{v}$. The second term $-r_{0,g} \cdot (\partial F_\alpha/\partial r_0)$ determines the plasma currents, which turns out to be associated with diamagnetic currents balancing pressure gradients. The moments of the distribution function can be calculated by using [4]

$$\int \mathrm{d}^3 v = \int_{-\infty}^{\infty} v_\parallel \int_0^{\infty} \mathrm{d}v_\perp v_\perp \int_0^{2\pi} \mathrm{d}\varphi_g,$$

where φ_g is the gyro angle. The densities are determined by

$$n_\alpha(r_0, B, \phi) = \int F_\alpha \mathrm{d}^3 v.$$

With these distribution functions, the densities are functions of (r_0, B, ϕ), which reflects the spatial dependencies of the constants of motion. This implies that the quasi-neutral electric potential is of the form

$$\phi = \hat{\phi}(r_0, B). \tag{15a}$$

More specifically, if we for illustration consider ions with a positive unit charge and negative charges carried by the electrons, quasi-neutrality in the plasma implies that the equation

$$n_+(r_0, B, \phi) = n_-(r_0, B, \phi) \tag{15b}$$

can be used as an approximation for the Poisson equation $\varepsilon_0 \nabla^2 \phi = q_e \cdot (n_+ - n_-)$, where q_e is the negative elementary charge of the electron. As is well known, the quasi-neutral solution has typically a high accuracy in the plasmas of interest here, apart from regions with vanishingly small plasma densities (sheath potentials can form in such regions). This quasi-neutral equation can only have a solution if there exists an implicit function of the form of equation (13a), i.e.$\phi = \hat{\phi}(r_0, B)$, if the distribution functions are determined by the three invariants in equation (14a). The derivatives of the implicit function can for given expressions of $n_+(r_0, B, \phi)$ and $n_-(r_0, B, \phi)$ be calculated from

$$\frac{\partial\hat{\phi}(r_0, B)}{\partial r_0} = -\frac{\partial(n_+ - n_-)/\partial r_0}{\partial(n_+ - n_-)/\partial\phi} \tag{15c}$$

and a corresponding formula for $\partial\hat{\phi}(r_0, B)/\partial B$. Assuming smoothness conditions, the implicit function theorem assures that these derivatives exist if $\partial(n_+ - n_-)/\partial\phi$ is finite, which is the typical situation (for instance, this is satisfied if $\partial F_\alpha/\partial\varepsilon < 0$ everywhere). With quasi-neutrality, the densities are functions of only (r_0, B), where

$$n_\alpha(r_0, B) \equiv n_\alpha[r_0, B, \hat{\phi}(r_0, B)] \equiv n(r_0, B)$$

and corresponding relations hold for other quantities. The dependence on B reflects the possibility for longitudinal confinement based on the magnetic mirror effect (an ambipolar potential sheath near the end walls also add to longitudinal confinement of electrons in mirrors). It has previously been demonstrated how experimental profiles for the density and the temperatures could be adjusted to the distribution functions with the aid of local Maxwellians distributions and Abel transforms. Often a local Maxwellian with a Boltzmann density distribution $n_e^{(0)}(r_0, B)\mathrm{e}^{-q_e\phi/k_BT_e(r_0,B)}$ is appropriate for the electrons in the plasma. Equation (13c) can be written as a response relation to an applied change in the electric potential governed by

$$\left(\frac{\partial n_-}{\partial r_0}\right)_{B,\phi} = \left(\frac{\partial n_+}{\partial r_0}\right)_{B,\phi} + \frac{\partial(n_+ - n_-)}{\partial\phi}\frac{\partial\hat{\phi}}{\partial r_0} \approx q_e\left(\frac{1}{k_BT_+} + \frac{1}{k_BT_-}\right)n\frac{\partial\hat{\phi}}{\partial r_0}, \tag{15d}$$

where the right end neglects the ion response and assumes nearly Boltzmann density distributions. An interpretation of this formula is that the radial dependencies of the electron density adjust to this formula as a 'plasma polarization' [6] response to an electric potential $\hat{\phi}(r_0, B)$ in the plasma, where the radial variations of $\hat{\phi}(r_0, B)$ can be externally controlled by biased potential plates. In the Baker–Hammel studies, a plasma motion enforces a transverse electric field in the plasma by the polarization mechanism. The scope is the opposite cause here, i.e. where an applied electric field enforces a plasma motion (a rotation in this case) by the plasma polarization mechanism. The potential jump near wall, i.e. the ambipolar potential, has to be considered for the biased potentials.

The perpendicular pressure is of the form

$$P_{\perp,\alpha}(r_0, B) = \int\frac{mv_\perp^2}{2}F_\alpha\mathrm{d}^3v = P_{\perp,\alpha}[r_0, B, \hat{\phi}(r_0, B)].$$

With this distribution function, the plasma current along the vacuum magnetic field is zero, while the perpendicular plasma current $\mathbf{j}_{\perp,\alpha} = q\int\mathbf{v}_\perp f_\alpha\,\mathrm{d}^3v$ is calculated from

$$\mathbf{j}_{\perp,\alpha} = -q\int\mathbf{v}_\perp r_{0,g}\frac{\partial F_\alpha}{\partial r_0}\mathrm{d}^3v.$$

The perpendicular current is thus associated with the 'gyro ripple' of the distribution function. The term F_α does not contribute to this current, since the gyro angle integral only contains oscillatory terms. Carrying out the velocity integrations leads to

$$\mathbf{j}_\alpha = \frac{\hat{\mathbf{B}}_\mathrm{v}}{B_\mathrm{v}}\times\frac{\partial P_{\perp,\alpha}(r_0, B, \phi)}{\partial r_0}\nabla r_0 = \frac{\hat{\mathbf{B}}_\mathrm{v}}{B_\mathrm{v}}\times\left[\frac{\partial P_{\perp,\alpha}(r_0, B)}{\partial r_0} - \frac{\partial\phi}{\partial r}\frac{\partial P_{\perp,\alpha}}{\partial\phi}\right]\nabla r_0.$$

The current is perpendicular to the vacuum magnetic field $\mathbf{B}_\mathrm{v}$ and has no component along ∇r_0. Summing up currents and perpendicular pressure tensor components from all charges, this expression approaches the force balance $\mathbf{j}\times\mathbf{B}_\mathrm{v}\to\nabla_\perp P_\perp$ [4], if the distribution functions are reasonably close to local Maxwellian distributions and the magnetic gradient drifts are small. Under similar conditions, we obtain [4]

$$\mu_0\mathbf{j}\to\nabla\times\left(-\frac{\beta}{2}\mathbf{B}_\mathrm{v}\right).$$

Here, $\beta = 2\mu_0P_\perp/B_\mathrm{v}^2$ is a local beta value and $\mathbf{B}_\mathrm{v}$ is the vacuum magnetic field. From this, the total divergence free magnetic field is given by

$$\mathbf{B} = \left(1 - \frac{\beta}{2}\right)\mathbf{B}_\mathrm{v} + \nabla W_\beta, \tag{16a}$$

where $\nabla^2W_\beta = \frac{1}{2}\mathbf{B}_\mathrm{v}\cdot\nabla\beta$ and W_β is therefore given by the Coulomb integral

$$W_\beta(\mathbf{x}) = -\frac{1}{8\pi}\int\frac{\mathbf{B}_\mathrm{v}(\mathbf{x})'\cdot\nabla'\beta(\mathbf{x})'}{|\,\mathbf{x}-\mathbf{x}'\,|}\mathrm{d}^3x'. \tag{16b}$$

A long-thin expansion for quadrupolar mirror fields for W_β has been derived in [5].

Finally, it may be instructive to see how the Baker–Hammel results [7] fit into our Vlasov system. For clarity we consider distributions of the form $F_\alpha = F_\alpha^{(0)}(\mu, r_0)\mathrm{e}^{-\varepsilon/k_BT(r_0)}$, and obtain for the mean velocities $\mathbf{u}_\alpha\equiv\mathbf{j}_\alpha/(q_\alpha n)$

$$\mathbf{u}_\alpha = \left[\frac{1}{q_\alpha n}\frac{\partial P_{\perp,\alpha}(r_0, B)}{\partial r_0} + \frac{\partial\hat{\phi}}{\partial r_0}\right]\frac{\mathbf{B}_\mathrm{v}\times\nabla r_0}{B^2}, \tag{17}$$

where the last term in the parenthesis corresponds to the $\mathbf{E}\times\mathbf{B}$ drift (although the pressure gradient term contributes to the mean velocity, it does not correspond to a drift of the guiding center). When the diamagnetic drifts can be neglected, we find the common drift $\mathbf{u}_\alpha\to(\mathbf{E}\times\mathbf{B})/B^2$ or the 'Hall effect' formula $\mathbf{E}+\mathbf{u}_\alpha\times\mathbf{B}\to 0$ (i.e. the Lorentz force vanishes in the rest frame of the plasma). This is the Baker and Hammel result for the electric field produced by the polarization mechanism [6] to facilitate a plasma motion across a magnetic field. The ambipolar sheath should be accounted for in the biasing design. It may be instructive to notice that the ambipolar sheath potential had no prominent influence on the Baker–Hammel experiments on a plasma beam penetrating a magnetic field. For the biased plate arrangements, this suggests, despite the presence of the ambipolar sheath near the wall, that the *potential variations* between various biased plates are mapped to a corresponding *potential variation* between flux surfaces in the confinement region, thereby producing a plasma rotation which is controlled by the biased potential plates.

The given formulas for the considered kind of Vlasov equilibria has a resemblance with a fluid approach based on a pressure profile of the form $P(r_0, B)$, combined with a quasi neutral electric field which includes the Hall effect [27]. In a fluid description, the potential $\hat{\phi}(r_0, B)$ in the plasma is an independent function which can be adjusted to the experimental situation. Heavy ion beam probes is an available method to measure the electric potential in a plasma.

7. Discussion

The model field we have calculated has singularities for $z = \pm c$, and could therefore only be relevant for some region $|z|\leqslant z_m$ with a finite mirror ratio where $z_m < c$. The model field in this confinement region with a finite mirror ratio of $R_m\approx 4$ could be approached by a continuous field generated by selection of 3D superconducting coils (these coils would

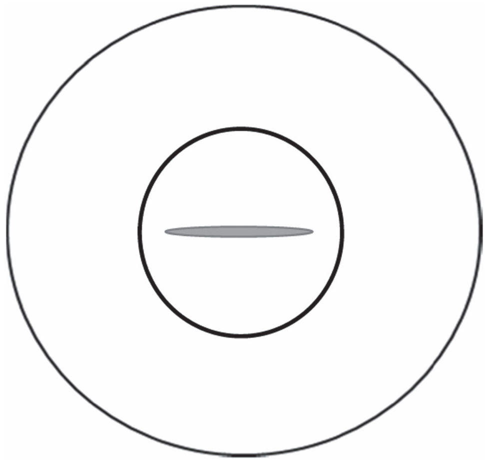

Figure 5. Qualitative cross sectional view near the mirror location with $R_m = 4$ with the parameters used in [25] for a hybrid reactor case. The inner circle corresponds to the vacuum chamber (radius 1 m). The cross section of the plasma surface, which is circular with a radius of 40 cm at the mid plane, has evolved to the elliptical cross section shown near the mirror location (the semi axis of the corresponding flux surface grows to 87 cm in the recirculation region beyond this location, but is still kept inside the vacuum chamber radius, see [25]. The outer circle in the figure corresponds to the inner radius (2.1 m) of the superconducting 'fish-bone' coils shown in figure 3. The outer radius of the coils (2.89 m, not shown in the above figure) is less than 3 m. The arrangements admit a sufficiently wide space (more than 1 m wide) for placing necessary elements of a reactor core in the annular region between the coil inner radii and the vacuum chamber. These elements include a 15 cm core expansion zone adjacent to the first wall, followed by a 22 cm wide region containing nuclear fuel and eutectic lead bismuth coolant, a neutron reflector region (about 50 cm wide), a tritium breeding region, with parameters consistent with the neutron computations in [20]. There is also space left for additional neutron shielding of the superconducting coils.

also generate the field in the flux expanding regions beyond the mirrors). Such coils have already been calculated for a more long-thin case, compare [25] where profiles of magnetic field components, field errors, cross sectional views etc are presented. Detailed parameter values in [25] are 2.1 m for the inner radii of the coils and 2.89 m for the coil outer radii. The vacuum chamber radius (1 m) is large enough to situate a plasma with a mid-plane radius of 0.4 m, where the flux tube evolves to an elliptical cross section near the magnetic field maxima. The cross section near the field maxima in figure 5 gives a qualitative view of the plasma shape near the mirror location. The compact 'fish bone' coils [25] shown in figure 3 provide sufficient space (more than 1 m wide) in the annular region bounded by the vacuum chamber and the inner coil radius for necessary reactor core elements.

Flute mode stability has been investigated both for a pressure peaking at the mid plane as well as for a sloshing ion distribution with density peaks located some distance apart from the midplane [25]. In the stability analysis, the pressure approaches zero outside the confinement region. The confinement region is considered to be a region with a magnetic field providing flute mode stability (by satisfying a pressure weighted average minimum B criterion). Another characterization of this confinement region is that each gyro center should move close to its mean magnetic surface (a radial electric field, in combination with an adequate magnetic field, could be beneficial to approach such a situation).

There is a class of particles in the warm plasma confined by the electric potential in between sloshing ion peaks. Longitudinal variations of the electric potential may also lead to more local trapping of Yushmanov ions, to a neighborhood of a local minimum of the guiding center potential $U_{\rm gc} = \mu B + q\phi$. A radial electric field of reasonable strength can supress radial excursions of such particles when the quasi-neutral potential is of the form $\hat{\phi}(r_0, B)$ (the corresponding drift would not lead to a net radial drift). Derivations are given in appendix D.

The flux tube cross section computed from the coil set evolves from a circular shape at the mid plane and compresses to a an elliptical shape near the field maxima, followed by an expansion beyond the mirrors with a nearly circular shape of the flux tube cross section near the end tank walls [25]. A nearly circular shape of the flux surface cross section at the end tank is obtained by magnetic shaping with appropriate coil parameters including a circular coil with a reversed current direction behind each end tank. The nearly circular flux tube cross section shape is revealed by the result that the function $g(z)$ in [25] approaches small values near these positions, compare figure 5(b) in [25]. The nearly circular shape enable arrangements of a large number of independently biased potential plates near the end tank walls. Typical electron gyro radii near the end tank wall are reasonably small (less than 1 cm), while the large ion gyro radii (about 50 cm) provide an evenly distributed heat load over the end tank wall areas (our design criteria for the heat load is less than 1 MW m^{-2} for a 1.5 GW hybrid reactor with 10 MW fusion power). The small ratio of the electron gyro radius to the end tank wall radius is an arrangement which may admit quite a detailed control of the radial variations of the electric potential in the confinement region. The goal is that the electric field should act like a 'glue' to force the ion center orbits closer to their mean magnetic surfaces.

The potential control relies on the plasma polarization mechanism [6], which needs a finite (although small) plasma density in a region near the end tank walls, where a potential change at biased plates is intended to propagate along field lines to the confinement region. An estimate on the density near the end tank wall for the plasma polarization to take place can be found from a condition that the electron plasma frequency $\omega_{pe} = \sqrt{q^2 n/(m_e \varepsilon_0)}$ has a larger magnitude than the cyclotron frequency $\Omega_e = qB/m_e$, i.e.

$$n[m^{-3}] > \frac{\varepsilon_0}{m_e} B^2 \approx 10^{19} \times B^2_{\text{end tank}}[T] \approx 2 \times 10^{15}\ \text{m}^{-3},$$

where in the last step we have considered an end tank wall radius around 4 m and a representative mid plane field strength of $B_0 = 1.25$ T. Densities well above such small values should be expected outside the confinement region (apart from the thin ambipolar sheath adjacent to the end tank walls). Radial drift loss exterior to the central confinement region is a selection mechanism between the regions, which could be viewed as an effect that defines the space for confinement. As shown in appendix D, omnigenous magnetic fields near the axis can be constructed in a transition region towards the expander region, which is bounded by the central confinement region and the maximal B on a flux surface. Therefore, neoclassical effects in the transition region may be limited to a small annular region, as depicted in figure 1. A rapid loss of ions in this annular region is not expected to be important for the overall power balance, in cases when the volume and particle number in this annular region is small. In the end tank region, power consumption is also expected to be small with adequate control of density and impurities.

Neoclassical effects could potentially be a threat for a class of particles appearing in the areas where the magnetic field strongly deviates from the straight-field-line shape. This is considered in appendix D. Yushmanov ions, which are longitudinally trapped in a region close to the mirror, can have large radial excursions due to magnetic drifts. Their number cannot be high since this area is small (see [23]). Furthermore, as shown in appendix D, the orbits of such particles could be cured by the radial electric field, as earlier shown for a much stiffer case with a magnetic mirror configuration corrupted by a stellarator field [24]. For a fusion reactor, a modest voltage difference (less than 1 kV) is estimated to be sufficient for a strong reduction of the radial excursions of Yushmanov ions (see appendix D). Thus, the essential neoclassical effects from Yushmanov ions and ions in the transition region may be limited to ions in a thin annular transition region, and their influence on the overall power and particle balance could be small.

Field errors, in particular the deviations from the calculated field and a field generated by coils, are presented in [25]. Such field errors would increase with a shorter device, where reproduction of the desired field gradients are harder to accomplish. Field errors give rise to magnetic drifts, which could result in loss of particles if no action is taken to cure this. A suggestion in this paper is that a radial electric field could be a tool to eliminate radial drift loss in quadrupolar mirrors, and thereby provide a higher margin on field errors. Field errors could be decreased substantially by shrinking the annular 'reactor region' filling the space between the vacuum tank and the inner coil radius, which would be an option for a stand alone fusion device, or even more so for a short device filled with an ordinary hydrogen plasma (i.e. no deuterium or tritium fuel) with the restricted aim to demonstration adequate plasma confinement.

When the gyro centers move close to their mean magnetic surfaces, a Vlasov description with the gyro center radial coordinate leads to a close resemblance with the magnetic field equations obtained from fluid approaches [23, 27]. A difference from the fluid models in [23, 27] is the addition of a quasi-neutral potential, where the Vlasov system is capable of modeling plasma rotation generated by the plasma polarization mechanism. This common $\mathbf{E} \times \mathbf{B}$ drift is not accompanied by an electric current for a quasi-neutral system, and the rotation has therefore no direct impact on the magnetic field.

Earlier studies have been investigating proper shaping of mirror fields for the reduction of radial magnetic drifts. An example is [23], where investigations are made for a tandem mirror with a nearly axisymmetric central cell. In [23], transition regions are treated with an aim to reduce neoclassical effects (compare also appendix D). The role of radial electric field is typically not covered as thoroughly as the magnetic field in earlier studies, which usually were dedicated to overcome neoclassical loss by magnetic field shaping. Combining optimal shapes of magnetic field with a controlled electric field may be a tool for further advancement in avoiding neoclassical loss [4, 24].

8. Conclusions

A vacuum magnetic field with minimal magnetic drifts has been derived to a higher order in a long-thin expansion. One purpose is to enable more 'short-fat' configurations, where the ratio of plasma radius a at the mid-plane to the length $2c$ could be increased. Previous derivations to a lower order may be adequate for $a/c < 0.1$, while inclusions of the higher order terms may admit extension of the parameter range up to $a/c < 0.3$. Design of superconducting magnetic coils for a shorter configuration can be based on the 3D superconducting coil design already computed for the longer device. With a plasma radius of 0.4 m, the length $2c$ could then be decreased to about 3 m.

The leading order solution has no magnetic drift, and each guiding center moves along a single magnetic field line. A slow magnetic drift is revealed by the higher order expansion terms, but the velocities of the magnetic drifts are exceptionally small (less than $1\ \mathrm{m\,s^{-1}}$ for particles with representative parameters for a fusion device). A first integral $\tilde{I}_r$ for the drift motion has been derived when only vacuum magnetic drifts are taken into account in the drift equations, and the constant $\tilde{I}_r$ applies to all particles in the drift ordering. The existence of the constant $\tilde{I}_r$ implies that all particles have a bounded radial motion. The constant $\tilde{I}_r$ corresponds to moderate radial excursions from the mean magnetic surface with a relative deviation of $\Delta r_0/r_0 \approx \pm 10\%$ along the guiding center orbits.

The radial excursions can be drastically reduced by adding a weak radial electric field. This is also expected to enable a higher tolerance towards magnetic field errors, with radial confinement maintained. The reduction in radial excursions is associated with the small ratio ε_E of the magnetic to the $\mathbf{E} \times \mathbf{B}$ drift along the poloidal direction. The reduction parameter ε_E can be controlled by electrically biased plates outside the confinement region, and exceptionally small potential variations are needed for this control in the considered magnetic mirror field. A configuration is identified where *each gyro center moves almost arbitrarily close to its mean magnetic surface*. This result is a motivation to use the gyro center radial coordinate as a constant of motion in a Vlasov description with a finite β. Vlasov equilibria are constructed based on the gyro center radial constant of motion, in addition to the conventional magnetic moment and energy invariants. Those Vlasov equilibria turn out to correspond to Hall fluid models based on pressure profiles in the form $P(r_0, B)$ combined with a quasi neutral electric potential in the form $\hat{\phi}(r_0, B)$, where the profiles can be fitted to an experimental situation. The Vlasov systems can flexibly model plasma rotations, where biased potentials offer a control tool. This plasma rotation can be associated with a plasma polarization mechanism, which was thoroughly investigated by Baker and Hammel for plasma flows across a magnetic field [6].

For the geometrical arrangements of biased plates, it is important to trace cross flux tube cross sections at the end tank. Short-circuiting between biased plates by the high electron mobility along magnetic field lines must be avoided. Radial electric fields of modest strength (voltage difference less 1 kV) has been considered in this paper. With adequate magnetic (with suitable coil arrangements) and electric field shaping, neoclassical effects are strong only for a limited population of ions located in a narrow annular transition region between the central confinement region and the expanders. The neoclassical effects are therefore expected to be minor.

Compared to axisymmetric mirrors, quadrupolar mirrors could have drawbacks on ellipticity, neoclassical effects, limited mirror ratios and more complex coils, and these obstacles need to be kept within a manageable range. Quadrupolar fields could be important for their stabilizing effect on the flute mode. Minimum B properties have been analyzed. All vacuum fields where the leading terms correspond to the SFLM field are found to violate the minimum B criterion, although the leading order solution corresponds to a marginal minimum B field. Since only the higher order terms are responsible for the violation of the minimum B criterion, the criterion is only 'mildly violated'. Other effects could therefore be sufficient to stabilize the mode. It is mentioned that wall stabilization and line tying improve the flute mode stability. Another robust option is to adjust the strength near the axis of a stabilizing quadrupolar field.

Acknowledgments

The reviewer is acknowledged for hard constructive work and emphasizing unclear points in the original manuscript, in particular on neoclassical effects and pit-falls related to a mismatch of biased plates and flux surface footprints on the end tank wall. Dr Marcus Berg is thanked for preparing figures 4 and D1. This work is dedicated to the late Professor Teruji Cho, former head of the Gamma10 experiments, for his lifelong contributions to mirror machine physics.

Appendix A

We derive the solution of S_1, S_2, $\bar{S}$ for the case $S_2 = S_1$. From that, it is straightforward to obtain the general equations that determine S_1, S_2, $\bar{S}$. With $c_1 = -c_2 = c > 0$, we find

$$\frac{\mathrm{d}}{\mathrm{d}z}\left[\left(\frac{T_1^2}{T_2^2} - \frac{T_2^2}{T_1^2}\right)\eta_0\right] = K \cdot \left[\frac{7(\Delta c)^2}{4}\left(\frac{1}{T_2^2} - \frac{1}{T_1^2}\right) + (\Delta c)^3\left(\frac{1}{T_2^3} + \frac{1}{T_1^3}\right)\right].$$

Integration leads to

$$\eta_0(z) = B_0 c^3 \cdot \frac{(c^2 - z^2)^2}{c^2 + z^2}\frac{1}{cz} \times \left[k_0 - \frac{7}{4}\frac{c^2}{c^2 - z^2} + c^2\frac{c^2 + z^2}{(c^2 - z^2)^2}\right],$$

where k_0 is a constant. The irregularity at $z = 0$ is avoided with $k_0 = 3/4$, and we obtain

$$\eta_0(z) = B_0 c^3\left(\frac{3}{4} + \frac{1}{2}\frac{c^2}{c^2 + z^2}\right) \cdot \frac{z}{c}.$$

This yield $\bar{S} = H_0$, where

$$H_0(z) = -\frac{1}{2}\frac{B_0}{c^4}\left(\frac{c^2}{c^2 + z^2}\right)^2.$$

We continue with a calculation of S_1 (z) from equations (5a)–(5c). We introduce $\tilde{c}^2 = c^2 - z^2$ and

$$g_T = \frac{T_1^2}{T_2^2} + \frac{T_2^2}{T_1^2} = \frac{2(c^4 + 6c^2z^2 + z^4)}{\tilde{c}^4}.$$

We then obtain

$$6(S_1 + S_2) = F_{H_0} + F_{\eta_0} + F_K,$$

$$F_{H_0} = -g_T H_0 = \frac{B_0}{c^4}\left(\frac{c}{\tilde{c}}\right)^4 \cdot \frac{c^4 + 6c^2z^2 + z^4}{(c^2 + z^2)^2},$$

$$F_{\eta_0} = \frac{\eta_0}{c^4\tilde{c}^2}\frac{\mathrm{d}g_T}{\mathrm{d}z} = \frac{B_0}{c^4}\left(\frac{c}{\tilde{c}}\right)^4 \cdot 8\frac{5c^2z^2 + 3z^4}{\tilde{c}^4},$$

$$F_K = -\frac{K}{c^4\tilde{c}^2}\left[\frac{3}{4}g_T - \frac{3}{2} + \frac{7(\Delta c)^2}{4}\left(\frac{1}{T_2^2} + \frac{1}{T_1^2}\right) + (\Delta c)^3\left(\frac{1}{T_2^3} - \frac{1}{T_1^3}\right)\right].$$

With

$$\frac{3}{4}g_T - \frac{3}{2} = \frac{12c^2}{\tilde{c}^4}$$

and $\Delta c = 2c$, we obtain $K = -B_0 c^2$ and

$$F_K = \frac{B_0}{c^4}\frac{c^2}{\tilde{c}^2}\left[\frac{12c^2z^2}{\tilde{c}^4} + 7c^2\frac{T_1^2 + T_2^2}{\tilde{c}^4} + 8c^3\frac{T_1^3 - T_2^3}{(T_1T_2)^3}\right].$$

With $T_1 = z + c$ and $T_2 = z - c$, we find

$$\frac{T_1^3 - T_2^3}{(T_1T_2)^3} = -\frac{2c(c^2 + 3z^2)}{\tilde{c}^6}.$$

Then

$$F_K = \frac{B_0}{c^4}\left(\frac{c}{\tilde{c}}\right)^4 \cdot \left[\frac{14c^2 + 26z^2}{\tilde{c}^2} - 16\frac{c^4 + 3c^2z^2}{\tilde{c}^4}\right].$$

With $S_2 = S_1$, we find

$$12S_1 = \frac{B_0}{c^4}\left(\frac{c}{\tilde{c}}\right)^4 \cdot \left\{\frac{c^4 + 6c^2z^2 + z^4}{(c^2 + z^2)^2} + R_1\right\},$$
$$R_1 = 8\frac{5c^2z^2 + 3z^4}{\tilde{c}^4} + \frac{14c^2 + 26z^2}{\tilde{c}^2} - 16\frac{c^4 + 3c^2z^2}{\tilde{c}^4}.$$

Some algebra results in $R_1 = -2$. Therefore the final formula $S_1 = H_0/6$ is recognized from

$$12S_1 = \frac{B_0}{c^4}\left(\frac{c}{\tilde{c}}\right)^4 \cdot \left[\frac{c^4 + 6c^2z^2 + z^4}{(c^2 + z^2)^2} - 2\right] = -\frac{B_0}{c^4}\left(\frac{c^2}{c^2 + z^2}\right)^2.$$

Appendix B. Arc length along *B* and modulus *B*

For the description of the guiding center motion, it may be instructive to compare the expressions for the strength of the magnetic field, if we replace the scalar magnetic potential coordinate with the arc length along the magnetic field lines. This arc length $s(\mathbf{x})$ obeys $\nabla s \cdot \hat{\mathbf{B}} = 1$, which in our vacuum field yields $\nabla s \cdot \nabla W = B$. With the long-thin expansion

$$s = z + \frac{x^2/2}{T_1} + \frac{y^2/2}{T_2} + x^4\gamma_1(z) + x^2y^2\bar{\gamma}(z) + y^4\gamma_2(z) + \mathrm{O}(\lambda^6) \tag{B1}$$

and the corresponding expansion for W, this leads to, when terms of order λ^6 are omitted:

$$B = \tilde{B}(z) + \frac{x^2}{2}\left(A_1' - \frac{\tilde{B}}{T_1^2} + 2\frac{A_1}{T_1}\right) + \frac{y^2}{2} \times \left(A_2' - \frac{\tilde{B}}{T_2^2} + 2\frac{A_2}{T_2}\right) + x^4p_1 + x^2y^2\bar{p} + y^4p_2,$$
$$p_i(z) = \left(\gamma_i' + \frac{4}{T_i}\gamma_i\right)\tilde{B} - \frac{1}{4}\frac{A_i'}{T_i^2} + \eta_i' + \frac{4}{T_i}\eta_i,$$
$$\bar{p}(z) = \left[\bar{\gamma}' + \left(\frac{2}{T_1} + \frac{2}{T_2}\right)\bar{\gamma}\right]\tilde{B} - \frac{1}{4}\left(\frac{A_1'}{T_2^2} + \frac{A_2'}{T_1^2}\right) + \bar{\eta}' + \left(\frac{2}{T_1} + \frac{2}{T_2}\right)\bar{\eta}.$$

A comparison with equations (2*g*), (2*h*) shows that $p_i(z) = P_i$ and $\bar{p}(z) = \bar{P}$, which amounts to

$$\frac{\mathrm{d}(T_i^4\gamma_i)}{\mathrm{d}z} = \frac{T_i^4}{4}\left[\frac{A_i'}{\tilde{B}T_i^2} - \frac{1}{T_i^4}\left(\frac{1}{2} + \frac{\tilde{B}A_i'}{A_i^2}\right)\right] = -\frac{1}{8},$$
$$\frac{\mathrm{d}(T_1^2T_2^2\bar{\gamma})}{\mathrm{d}z} = \frac{T_1^2T_2^2}{4}\left[\frac{1}{\tilde{B}}\left(\frac{A_1'}{T_2^2} + \frac{A_2'}{T_1^2}\right) - \frac{1}{T_1^2T_2^2} \times \left(1 + \frac{\tilde{B}A_1'}{A_1^2} + \frac{\tilde{B}A_2'}{A_2^2}\right)\right] = -\frac{1}{4}.$$

With $c_2 = -c_1 = -c$ and with k_1, $\bar{k}$, k_2 constants, γ_1, $\bar{\gamma}$, γ_2 are integrated to

$$\gamma_1(z) = -\frac{1}{8}\frac{z + k_1}{(c + z)^4}, \tag{B2a}$$
$$\gamma_2(z) = -\frac{1}{8}\frac{z + k_2}{(c - z)^4}, \tag{B2b}$$
$$\bar{\gamma}(z) = -\frac{1}{4}\frac{z + \bar{k}}{(c^2 - z^2)^2}. \tag{B2c}$$

The expression for the arc length becomes with $\tilde{x}_0 = \frac{cx}{c+z}$ and $\tilde{y}_0 = \frac{cy}{c-z}$:

$$s = z + \frac{1}{2}\left(\frac{x^2}{c + z} - \frac{y^2}{c - z}\right) - \frac{z + k_1}{8}\frac{\tilde{x}_0^4}{c^4} - \frac{z + \bar{k}}{4}\frac{\tilde{x}_0^2\tilde{y}_0^2}{c^4} - \frac{z + k_2}{8}\frac{\tilde{y}_0^4}{c^4}. \tag{B2d}$$

The values of the constants k_1, $\bar{k}$, k_2 have an influence on the shape of the surface $s(\mathbf{x}) = 0$. It can be noticed that the arc length somewhat surprisingly has a common expression given by equation (B2*d*) in the considered magnetic fields, which is valid for all choices of the 'generator'$\eta(z)$. A check shows that the leading order terms correspond to $\nabla s \to \hat{\mathbf{B}}$, but that $|\nabla s| > 1$ when higher order terms are included, and thus ∇s also contains components perpendicular to $\hat{\mathbf{B}}$. Apart from corrections of order λ^6, equation (B2*d*) gives

$$|\nabla s| = 1 + \frac{1}{4}\frac{r_0^4}{c^4}$$

which confirms that the higher order terms give $|\nabla s| > 1$. With the choice $k_1 = \bar{k} = k_2$, the expression for the arc length becomes particularly compact:

$$s \to z + \frac{1}{2}\left(\frac{x^2}{c + z} - \frac{y^2}{c - z}\right) - \frac{z + k_1}{8}\frac{(\tilde{x}_0^2 + \tilde{y}_0^2)^2}{c^4}.$$

In this form, the higher order corrections to the arc length are zero at the plane $z = -k_1$.

We continue with a derivation of an expression for B in the variables x_0, y_0, s. We neglect terms of order λ^6 and start from

$$B(x_0, y_0, s) = \breve{B}\,[W(x_0, y_0, s)] + x_0^4S_1(s) + x_0^2y_0^2\bar{S}(s) + y_0^4S_2(s),$$

where, with $\tilde{B}(z) = \breve{B}[\tilde{W}(z)]$:

$$\breve{B}(W) = \tilde{B}(z) + (W - \tilde{W})\frac{1}{\tilde{B}(z)}\frac{\mathrm{d}\tilde{B}(z)}{\mathrm{d}z} + \frac{(W - \tilde{W})^2}{2}\frac{1}{\tilde{B}}\frac{\mathrm{d}}{\mathrm{d}z}\left(\frac{1}{\tilde{B}}\frac{\mathrm{d}\tilde{B}}{\mathrm{d}z}\right).$$

The first term on the rhs is expressed in the arc length by using

$$\tilde{B}(z) = \tilde{B}(s) - (s - z)\frac{\mathrm{d}\tilde{B}(z)}{\mathrm{d}z} + \frac{(s - z)^2}{2}\frac{\mathrm{d}^2\tilde{B}(z)}{\mathrm{d}z^2},$$

where $\tilde{B}(s) = B_0/(1 - s^2/c^2)$. Combining these three equations result in

$$B = \tilde{B}(s) + [(W - \tilde{W}) - (s - z)\tilde{B}]\frac{1}{\tilde{B}}\frac{\mathrm{d}\tilde{B}}{\mathrm{d}z} + \frac{(W - \tilde{W})^2}{2}\frac{1}{\tilde{B}}\frac{\mathrm{d}}{\mathrm{d}z}\left(\frac{1}{\tilde{B}}\frac{\mathrm{d}\tilde{B}}{\mathrm{d}z}\right) + \frac{(s - z)^2}{2} \times \frac{\mathrm{d}^2\tilde{B}(z)}{\mathrm{d}z^2} + x_0^4 S_1(s) + x_0^2 y_0^2 \bar{S}(s) + y_0^4 S_2(s).$$

Using the expansions (B1) and (2a) with equations (3a), (3b), (3f), (3g), (5d) and (7a), (7b) add up to

$$B(x_0, y_0, s) = \tilde{B}(s) + x_0^4\Gamma_1(s) + x_0^2 y_0^2\bar{\Gamma}(s) + y_0^4\,\Gamma_2(s),$$

$$\Gamma_1 = S_1 + \frac{z}{c^4\tilde{c}^4}\frac{T_1^2}{T_2^2}\frac{\eta}{3} + \frac{B_0}{c^2}\left[\frac{z(z + k_1)}{4\tilde{c}^4} - \frac{z}{3}\frac{c^2 - 2cz + 3z^2}{T_1 T_2^4} - \frac{c^2 + 2z^2}{2T_1 T_2^3}\right],$$

$$\Gamma_2 = S_2 + \frac{z}{c^4\tilde{c}^4}\frac{T_2^2}{T_1^2}\frac{\eta}{3} + \frac{B_0}{c^2}\left[\frac{z(z + k_2)}{4\tilde{c}^4} - \frac{z}{3}\frac{c^2 - 2cz + 3z^2}{T_1^4 T_2} - \frac{c^2 + 2z^2}{2T_1^3 T_2}\right],$$

$$\bar{\Gamma} = \bar{S} - \frac{2s}{c^4\tilde{c}^4}\eta + \frac{B_0}{c^2}\frac{1}{\tilde{c}^4}\left[\frac{(z + \bar{k})z}{2} - c^2 - 2z^2\right].$$

These formulas demonstrates that $\Gamma_i \neq S_i$ and $\bar{\Gamma} \neq \bar{S}$, which are connected with the components perpendicular to $\hat{\mathbf{B}}$ of ∇s. The connection to the formulas with the scalar magnetic potential can be interpreted from the integral relation between the scalar magnetic potential of a vacuum field and the arc length;

$$W(x_0, y_0, s) = \int_{s_0(x_0,y_0)}^{s} B(x_0, y_0, s')\,\mathrm{d}s'$$

or $(\partial W/\partial s)_{x_0,y_0} = B$, which leads to

$$\nabla s = \hat{\mathbf{B}} - \frac{1}{B}\frac{\partial W}{\partial x_0}\nabla x_0 - \frac{1}{B}\frac{\partial W}{\partial y_0}\nabla y_0.$$

The components perpendicular to $\hat{\mathbf{B}}$ is recognized from the two last terms. In our case, it turns out that the arc length is not the most convenient variable to describe the drift motion. The scalar magnetic potential is more suitable when higher order expansion terms are included.

Appendix C. Clebsch coordinates

We make the expansion

$$x_0 = \frac{cx}{c + z}[1 + a_1(z)x^2 + b_1(z)y^2] + \mathrm{O}(\lambda^5),$$

$$y_0 = \frac{cy}{c - z}[1 + a_2(z)y^2 + b_2(z)x^2] + \mathrm{O}(\lambda^5)$$

Then the Cartesian components of $\mathbf{B} = B_0\nabla x_0 \times \nabla y_0$ yield

$$B_x = \frac{x \cdot \tilde{B}(z)}{c + z}(1 + x^2\varepsilon_{xx} + y^2\varepsilon_{xy}) + \mathrm{O}(\lambda^5),$$

$$B_y = -\frac{y \cdot \tilde{B}(z)}{c - z}(1 + x^2\varepsilon_{yx} + y^2\varepsilon_{yy}) + \mathrm{O}(\lambda^5),$$

$$B_z = \tilde{B}(z)(1 + x^2\varepsilon_{zx} + y^2\varepsilon_{zy}) + O(\lambda^4),$$

where $\tilde{B}(z) = B_0/(1 - z^2/c^2)$ and

$$\varepsilon_{xx} = a_1 - (c + z)a_1' + b_2$$

$$\varepsilon_{xy} = 3a_2 + \left[1 + 2\frac{c + z}{c - z} - (c + z)\frac{\mathrm{d}}{\mathrm{d}z}\right]b_1,$$

$$\varepsilon_{yx} = 3a_1 + \left[1 + 2\frac{c - z}{c + z} + (c - z)\frac{\mathrm{d}}{\mathrm{d}z}\right]b_2,$$

$$\varepsilon_{yy} = a_2 + (c - z)a_2' + b_1,$$

$$\varepsilon_{zx} = 3a_1 + b_2,$$

$$\varepsilon_{zy} = 3a_2 + b_1.$$

Two of these equations are dependent in view of $\nabla \cdot \mathbf{B} = 0$, which implies:

$$0 = \frac{3\varepsilon_{xx}}{c + z} - \frac{\varepsilon_{yx}}{c - z} + \frac{1}{\tilde{B}}\frac{\mathrm{d}(\tilde{B}\varepsilon_{zx})}{\mathrm{d}z},$$

$$0 = \frac{\varepsilon_{xy}}{c + z} - \frac{3\varepsilon_{yy}}{c - z} + \frac{1}{\tilde{B}}\frac{\mathrm{d}(\tilde{B}\varepsilon_{zy})}{\mathrm{d}z}.$$

Using these divergence free relations and the substitutions $b_2 = -3a_1 + \varepsilon_{zx}$ and $b_1 = -3a_2 + \varepsilon_{zy}$, the second equation becomes identical to the 4th equation, while the third equation is identical to the first equation. The first and 4th equations result in

$$\frac{\mathrm{d}[(c + z)^2 a_1]}{\mathrm{d}z} = -(c + z)(\varepsilon_{xx} - \varepsilon_{zx}),$$

$$\frac{\mathrm{d}[(c - z)^2 a_2]}{\mathrm{d}z} = (c - z)(\varepsilon_{yy} - \varepsilon_{zy}).$$

For the considered magnetic field, we have from equations (10d)–(10f)

$$(c + z)(\varepsilon_{xx} - \varepsilon_{zx}) = (c - z)(\varepsilon_{yy} - \varepsilon_{zy}) = -\frac{1}{6}\frac{c}{c^2 + z^2}.$$

We then find with $a_i(0) = 0$:

$$a_1(z) = \frac{1}{6}\frac{\tan^{-1}\left(\frac{z}{c}\right)}{(c + z)^2},\quad a_2(z) = -\frac{1}{6}\frac{\tan^{-1}\left(\frac{z}{c}\right)}{(c - z)^2}.$$

Explicit formulas for the Clebsch coordinates are with $\tilde{x}_0 = \frac{cx}{c+z}$ and $\tilde{y}_0 = \frac{cy}{c-z}$:

$$x_0 = \tilde{x}_0 \cdot \left\{1 + \frac{\tilde{x}_0^2}{6c^2}\tan^{-1}\left(\frac{z}{c}\right) + \frac{\tilde{y}_0^2}{2c^2}\left[-\frac{c+3z}{c+z} + \tan^{-1}\left(\frac{z}{c}\right)\right]\right\},$$

$$y_0 = \tilde{y}_0 \cdot \left\{1 + \frac{\tilde{x}_0^2}{2c^2}\left[-\frac{c-3z}{c-z} - \tan^{-1}\left(\frac{z}{c}\right)\right] - \frac{\tilde{y}_0^2}{6c^2}\tan^{-1}\left(\frac{z}{c}\right)\right\}.$$

Appendix D. Yushmanov and transition region ions and end tank flux tube footprints

The magnetic field deviate substantially from the ideal field calculated in a region where the flux tube expands, and these field deviations have implications on radial drifts and neoclassical transport. We therefore consider to leading order effects on radial confinement from strong deviations from the ideal field. Assume quadrupolar symmetry and consider leading paraxial expressions: we analyze a symmetrical quadrupolar field satisfying $\tilde{B}(-z) = \tilde{B}(z)$. Since $\tilde{B}(z) = \frac{B_0}{[1+\gamma_1(z)][1+\gamma_2(z)]}$, this yields $\gamma_2(z) = \gamma_1(-z)$. This is satisfied with $\gamma_1(z) = \gamma_e(z) + \gamma_o(z)$ and $\gamma_2(z) = \gamma_e(z) - \gamma_o(z)$, where $\gamma_e(z) = \gamma_e(-z)$ is an even function in z while $\gamma_o(z) = -\gamma_o(-z)$ is an odd function in z. With $\gamma_e(0) = \gamma_o(0) = 0$, the field lines are expressed by

$$x(z) = [1 + \gamma_e(z) + \gamma_o(z)]x_0 + O(\lambda^3), \tag{D1a}$$

$$y(z) = [1 + \gamma_e(z) - \gamma_o(z)]y_0 + O(\lambda^3). \tag{D1b}$$

Equations (2b) and (4c) give for the magnetic field strength near the axis

$$\tilde{B}(z) = \frac{B_0}{(1+\gamma_e)^2 - \gamma_o^2}. \tag{D2}$$

A finite $\tilde{B}(z)$ implies $\gamma_o^2 < (1+\gamma_e)^2$. Axisymmetric fields have $\gamma_o(z) \equiv 0$ and $\gamma_e(z) \leqslant 0$ in the confinement region. For quadrupolar fields, $|\gamma_o(z)| \gg |\gamma_e(z)|$ in the confinement region, but in the flux expanding region beyond the mirrors,$\gamma_e(z)$ grows to a large value near the end tank [i.e. $(1+\gamma_e)^2 \to B_0/B_{\text{end tank}} \approx 100$], while $\gamma_o(z)/(1+\gamma_e)$ decreases to small values (this ensures a nearly circular flux tube cross section near the end tank walls). To analyze the guiding center orbit, we need the modulus of B: From equations (2k) and (4c) follow $B = \breve{B}(W) + B_{\text{rest}}$, where

$$B_{\text{rest}} = \tilde{B}(z)\left(\frac{x^2}{2}\frac{\gamma_e'' + \gamma_o''}{1+\gamma_e+\gamma_o} + \frac{y^2}{2}\frac{\gamma_e'' - \gamma_o''}{1+\gamma_e-\gamma_o}\right).$$

Therefore, near the axis, this becomes with $u_e(z) = 1 + \gamma_e$:

$$B(x_0, y_0, W) = \breve{B}(W)\left[1 + \frac{x_0^2}{2}(u_e+\gamma_0)(\gamma_e''+\gamma_o'') + \frac{y_0^2}{2}(u_e-\gamma_0)(\gamma_e''-\gamma_o'')\right].$$

Here, we can to leading order identify $\gamma_e(z)$ and $\gamma_o(z)$ as functions of W. In the variables (r_0, θ_0, W), we find

$$B(r_0, \theta_0, W) = \breve{B}(W)\left\{1 + \frac{r_0^2}{2}[u_e\gamma_e'' + \gamma_o\gamma_o'' + (\gamma_o\gamma_e'' + u_e\gamma_o'')\cos 2\theta_0]\right\}. \tag{D3}$$

An inspection of this formula reveals that no magnetic radial drifts appear near the mid plane. To analyze the drifts, we assume an electric potential of the form $\hat{\phi}(r_0, B)$, which is consistent with quasy neutrality for a configuration where guiding centers move close to their mean magnetic surfaces. The guiding center orbits in the equilibrium are constrained by a constant energy $\varepsilon = U(r_0, B) + mv_\parallel^2/2$, where $U = q\hat{\phi}(r_0, B) + \mu B$ is the guiding center potential. Equation (1) then leads to

$$\dot{r}_0 = -\frac{1}{qB_0}\frac{1}{r_0}\frac{\partial B}{\partial\theta_0}\left(\frac{\partial U}{\partial B} + \frac{mv_\parallel^2}{B}\right),$$

$$r_0\dot{\theta}_0 = \frac{1}{B_0}\frac{\partial\hat{\phi}(r_0, B)}{\partial r_0} + \frac{1}{qB_0}\frac{\partial B}{\partial r_0}\left(\frac{\partial U}{\partial B} + \frac{mv_\parallel^2}{B}\right),$$

$$\dot{W} = Bv_\parallel.$$

The special case $\partial\hat{\phi}(r_0, B)/\partial r_0 = 0$ yields with the help of equation (D3)

$$\left.\frac{dr_0}{d\theta_0}\right|_{\frac{\partial\hat{\phi}}{\partial r_0}=0} = -\frac{\partial B/\partial\theta_0}{\partial B/\partial r_0} = r_0\frac{(\gamma_o\gamma_e'' + u_e\gamma_o'')\sin 2\theta_0}{u_e\gamma_e'' + \gamma_o\gamma_o'' + (\gamma_o\gamma_e'' + u_e\gamma_o'')\cos 2\theta_0}.$$

To estimate what this means, we consider a quadrupolar field region near the mirror. A first inspection of a case where $\gamma_e \to 0$ and $|\gamma_o| < 1$ would lead to

$$\left.\frac{dr_0}{d\theta_0}\right|_{\frac{\partial\hat{\phi}}{\partial r_0}=0} \to r_0\frac{\sin 2\theta_0}{\gamma_o + \cos 2\theta_0}.$$

However, the right-hand side then becomes singular for angles satisfying $\cos 2\theta_0 = -\gamma_o$. A more rigorous analysis is obtained by keeping γ_e finite and making the substitution

$$1 - \varepsilon_\gamma(z) = \sigma(z)\frac{\gamma_o\gamma_e'' + u_e\gamma_o''}{u_e\gamma_e'' + \gamma_o\gamma_o''}.$$

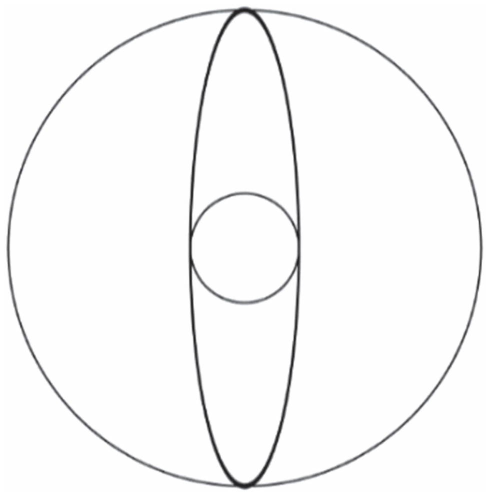

Figure D1. Contour of a Yushmanov ion gyro center orbit in the x_0y_0 plane, where radial electric fields are neglected. These guiding center orbits satisfy the equation $r_0 = I_Y \cdot [1 \pm (1-\varepsilon_\gamma)\cos 2\theta_0]^{-1/2}$, where I_Y is constant. The corresponding ion drift occur in a region bounded by the flux surfaces $(2-\varepsilon_\gamma)^{-1/2} \leqslant \frac{\bar{r}_0}{I_Y} \leqslant \varepsilon_\gamma^{-1/2}$, where the cross sections in the x_0y_0 plane of the bounding flux surfaces are the two circles shown in the figure. The outer flux surface is outside the plasma confinement region if ε_γ is sufficiently small. With an added radial electric field of moderate strength, the gyro motion of the corresponding ions is predicted to be restricted to a motion close to a single magnetic surface.

Here, $\sigma(z) = \pm 1$ have different sign on opposite sides of the mirror. This leads to

$$\left.\frac{\mathrm{d}r_0}{\mathrm{d}\theta_0}\right|_{\frac{\partial\hat{\phi}}{\partial r_0}=0} = r_0 \frac{\sigma(z)(1-\varepsilon_\gamma)\sin 2\theta_0}{1+\sigma(z)(1-\varepsilon_\gamma)\cos 2\theta_0}. \tag{D4a}$$

A class of ions (Yushmanov ions) can be longitudinally confined to a region where the magnetic field increases towards the mirror if the electric potential decreases along the same direction. For a nearly Boltzmann density distribution, this decrease in $\hat{\phi}(r_0, B)$ would be a consequence of a decreasing density towards the mirror region. If the longitudinal bounce is short enough, we may take $\varepsilon_\gamma(z)$ as a positive definite constant, and in such a case we obtain the first integral

$$I_Y = r_0 \cdot \sqrt{1 \pm (1-\varepsilon_\gamma)\cos 2\theta_0} = \text{constant}. \tag{D4b}$$

A case with $\varepsilon_\gamma \ll 1$ leads to substantial radial excursions, where the Yushmanov ions could drift across the flux surface which is intended to define the plasma boundary, as illustrated in figure D1. Such ions would be lost from confinement.

Let us investigate how the situation is changed when a radial electric field is added. With a sufficiently strong radial electric field applied, we again use the small parameter

$$\varepsilon_E = \frac{\left(\dfrac{\partial U}{\partial B} + \dfrac{mv_\parallel^2}{B}\right)\dfrac{1}{q}\dfrac{\partial B}{\partial r_0}}{\partial\hat{\phi}(r_0, B)/\partial r_0}.$$

In this case, this parameter is estimated by $\varepsilon_E \approx \varepsilon_E^{(0)} \cdot [1 + \sigma(z)(1-\varepsilon_\gamma)\cos 2\theta_0]$, where

$$\varepsilon_E^{(0)} \approx \frac{\frac{1}{q}\left(\frac{\partial U}{\partial B} + \frac{mv_\parallel^2}{B}\right)}{\partial\hat{\phi}(r_0, B)/\partial r_0} r_0 B \cdot (1+\gamma_0)\gamma_o''.$$

Here, radial drifts are oscillatory obeying an evolution equation which scales as

$$\frac{\mathrm{d}r_0}{\mathrm{d}\theta_0} \approx \varepsilon_E^{(0)} r_0 \sin 2\theta_0.$$

With a radial electric field applied, the amplitude of the radial excursions of the Yushmanov ions are therefore expected to shrink considerably; the ratio between the amplitudes is less than $|\varepsilon_E^{(0)}|$. To see what range of electric potential variations would be required for this, we obtain as an order of magnitude estimate,

$$|\varepsilon_E^{(0)}| \approx \frac{T_i(\mathrm{eV})}{|\Delta\phi|}\frac{r_0^2}{c^2}.$$

With the representative parameters $T_i(\mathrm{eV}) = 20$ keV, $\bar{r}_0 = 1$ m and $c = 50$ m for a full scale fusion device, this gives with $|\varepsilon_E^{(0)}| = 0.01$

$$|\Delta\phi| \approx \frac{1}{|\varepsilon_E^{(0)}|}\frac{r_0^2}{c^2} T_i(\mathrm{eV}) < 1\ \mathrm{kV}. \tag{D5}$$

A potential variation less than 1 kV can conveniently be handled, and such potential variations may be able to transform even these Yushmanov ion orbits (which may be close to 'worst case orbits') into an ion motion restricted to a neighborhood of the mean magnetic surface. The potential variation needs only to be strong enough to counteract the magnetic radial drifts (which are much smaller than the gyrating velocities). As expected, the strength of the required potential variation is therefore much lower than the temperature measured in electronvolts, i.e. $|\Delta\phi(\mathrm{V})| \ll T_i(\mathrm{eV})$ or $|q\Delta\phi| \ll k_B T_i$, which is in agreement with equation (D5).

Let us finally show that it is possible to find flux expanding fields which are omnigenous to leading order in the long-thin expansion. The omnigenuity condition for a quadrupolar field is, see [1, 2, 22] or equation (20*b*) in [5]

$$\gamma_o u_e'' + u_e \gamma_o'' = 0.$$

We can make our point by simply considering an odd function γ_o which results in $\gamma_o''/\gamma_o < 0$, whereby the omnigenuity equation results in an even function u_e which increases with the distance from the mid-plane. One such choice is $\gamma_o = \frac{z/c}{1+\alpha z^2/c^2}$, which approaches the SFLM field near the midplane when α is a positive constant. We then obtain

$$\frac{\gamma_o''}{\gamma_o} = -\frac{6\alpha}{c^2}\frac{1-\frac{\alpha}{3}\frac{z^2}{c^2}}{\left(1+\alpha\frac{z^2}{c^2}\right)^2}.$$

This quantity is slowly varying if α is not too large. A WKB solution to the omnigenuity equation with the Cauchy conditions $u_e(0) = 1$ and $u_e'(0) = 0$ results in

$$u_e = \frac{\sqrt{1 + \alpha\frac{z^2}{c^2}}}{\left(1 - \frac{\alpha}{3}\frac{z^2}{c^2}\right)^{1/4}} \cosh\left(\sqrt{6\alpha} \cdot \int_0^z \frac{\sqrt{1 - \frac{\alpha}{3}\frac{z^2}{c^2}}}{1 + \alpha\frac{z^2}{c^2}} \frac{\mathrm{d}z}{c}\right) \approx \cosh\left(\sqrt{6\alpha} \cdot \frac{z}{c}\right).$$

At the end tank wall, we have $u_e \approx \sqrt{B_0/B_{\text{end tank}}} \approx 10$, which is satisfied with $z/c \approx 1.2/\sqrt{\alpha}$, which suggests that the end tank region could be made short with an appropriate coil set (the case $\alpha = 1$ gives $z/c \approx 1.2$). The flux tube cross sections near the end tank wall is slightly disturbed from circles, and is in a paraxial approximation of the vaucum field determined by constant values of

$$r_0 \rightarrow \frac{r}{u_e}\left(1 - \frac{\gamma_0}{u_e}\cos 2\theta\right) \approx \frac{r}{M}\left(1 - \frac{\gamma_0}{M}\cos 2\theta\right).$$

Here, $M = \sqrt{B_0/B_{\text{end tank}}} \approx 10$ stands for the 'flux tube magnification' from the mid plane to the end tank. The mismatch from perfect circles of the flux tube cross sections at the end tank can be estimated from this formula. The formula also describes how flux conservation implies that a mid-plane plasma radius $a = 0.4$ m corresponds to an end tank flux tube radius $r \approx Ma = 4$ m when $B_0/B_{\text{end tank}} \approx 100$.

When a flux surface with a constant r_0, where $0 \leqslant r_0 \leqslant a$ for the confinement region, is mapped to the end tank, the long-thin approximation predicts that the radial coordinate at the end tank for the mapped flux footprint is bounded by the annular domain

$$M \cdot r_0 - \Delta r < r < M \cdot r_0 + \Delta r,$$

where $\Delta r \approx \gamma_0 r_0 \leqslant \gamma_0 a$. Twice this width, i.e.$2\Delta r$, is a minimum for each electric insulation width at the end tank if biased plates with circular boundaries would be used. A possibility for the possible biased plate arrangement is to use a set of annular circular plates (the central potential plate where the magnetic axis intersect could be a circle). Short-circuiting can be avoided with a sufficiently wide insulation distance Δr_{ins} between adjacent plates (the opposite end tank wall can be equipped with the same arrangement, but an even simpler solution may be to use insulation materials throughout that end tank surface). The formula above predicts that short-circuiting could be avoided if $\Delta r_{\text{ins}} \geqslant 2\gamma_0 a$, where the lower limit is approached for biased plates with a thin radial width. If there are N biased end plates, the added insulation distances must be smaller than the end tank radius Ma, i.e.

$$N\Delta r_{\text{ins}} \leqslant Ma,$$

where equality is approached for biased plates with a small width. This suggests that the maximum number of biased plates can be estimated by the integer part of

$$N \approx \frac{M}{2\gamma_0}.$$

A shaping of the magnetic field to low values of γ_0 at the end tank is essential to admit a large number of biased potentials and a more detailed control of the radial electric field in the confinement region. Cases with $N > 10$ (or even substantially larger) could be envisioned with parameter regimes relevant for a compact demonstration device. In addition to the radial resolution, there is also flexibility to vary the potential strengths during operation, where considerably higher voltages than 1 kV may be an interesting option for the studies.

References

[1] Catto P J and Hazeltine R D 1981 *Phys. Fluids* **24** 1663
[2] Ryutov D D and Stupakov G V 1987 *Reviews of Plasma Physics* vol 13 ed B B Kadomtsev (New York: Consultants Bureau) p 93
[3] Hall L S and McNamara B 1975 *Phys. Fluids* **18** 552
[4] Hinton F L and Hazeltine R D 1976 *Rev. Mod. Phys.* **48** 239
[5] Ågren O and Moiseenko V E 2014 *Plasma Phys. Control. Fusion* **56** 095026
[6] Baker D A and Hammel J E 1964 *Phys. Fluids* **8** 713
[7] Ågren O and Savenko N 2004 *Phys. Plasmas* **11** 5041
[8] Ågren O, Moiseenko V E and Savenko N 2005 *Phys. Rev.* E **72** 026408
[9] Furth H P and Rosenbluth M N 1964 *Phys. Fluids* **7** 764
[10] Koidan V S *et al* 2003 *Fusion Sci. Technol.* **43** 30
[11] Cho T *et al* 2006 *Phys. Rev. Lett.* **97** 055001
[12] Beklemishev A, Bagryansky P, Chashin M and Soldatkina E 2010 *Fusion Sci. Technol.* **57** 351
[13] Beklemishev A, Anikeev A, Burdakov A, Ivanov A, Ivanov I, Postupaev V and Sinitsky S 2012 *AIP Conf. Proc.* **1442** 147
[14] Bagryansky P A *et al* 2015 *Nucl. Fusion* **55** 053009
[15] Ryutov D D 1988 *Sov. Phys.—Usp.* **31** 301 (in Russian)
[16] Gott Y V, Ioffe M S and Tel'kovskii V G 1976 *Phys. Rev. Lett.* **36** 1051
[17] Moiseenko V E and Ågren O 2005 *Phys. Plasmas* **12** 102504
[18] Ågren O and Savenko N 2005 *Phys. Plasmas* **12** 022506
[19] Kotelnikov I A and Rome M 2012 *Phys. Plasmas* **19** 122509
[20] Noack K, Moiseenko V E, Ågren O and Hagneståł A 2011 *Ann. Nucl. Energy* **38** 578
[21] Ågren O, Moiseenko V E, Noack K and Hagneståł A 2010 *Fusion Sci. Technol.* **57** 326
[22] Skovoroda A A 1987 *Sov. J. Plasma Phys.* **13** 531
[23] Stupakov G V 1979 *Sov. J. Plasma Phys.* **5** 486
Stupakov G V 1979 *Fiz. Plazmy* **5** 871
[24] Moiseenko V E, Nemov V V, Ågren O, Kasilov S V and Garkusha I E 2016 *Plasma Phys. Control. Fusion* **58** 064005
[25] Hagneståł A, Ågren O and Moiseenko V E 2012 *J. Fusion Energy* **31** 379
[26] Northrop T and Teller E 1960 *Phys. Rev.* **117** 215
[27] Pearlstein L D, Kaiser T B and Newcomb W A 1981 *Phys. Fluids* **27** 1326